JOURNAL OF MATERIALS SCIENCE 20 (1985) 114–140

The mechanical response of glutaraldehyde-fixed bovine pericardium to uniaxial load

E. A. TROWBRIDGE, M. M. BLACK, C. L. DANIEL
Department of Medical Physics and Clinical Engineering, Sheffield University, The Royal Hallamshire Hospital, Sheffield, UK

Bovine pericardium, treated with glutaraldehyde, is used in the construction of heart valve substitutes. This study examines the mechanical properties of this tissue by using a continuum physics approximation of the material. A consideration of the relative magnitudes of the characteristic deformation time of a heart valve leaflet and the measured relaxation time of the tissue suggests that it can be effectively represented by a non-linear elastic solid. A compressible isotropic strain energy function is used to characterize the homogeneous deformation of the tissue when it is subjected to uniaxial load. The initial elastic material which is characterized by only two elastic constants, undergoes a transition to a second elastic material which is governed by a strain energy function of different magnitude by the same functional form as that associated with the initial elastic solid. This model is used to investigate the pericardial sac-to-sac and within-sac directional variation of the response to load in the unstrained state. Analysis of variance shows that glutaraldehyde treated pericardium possesses no preferred directional strength properties in the unstrained state. Any observed differences in the mechanical properties of different test specimens can be attributed to random biological variation alone.

1. Introduction and historical background

This study arises from the need to characterize the mechanical properties of bovine pericardium which is to be used in the construction of a heart valve. The design of a valve leaflet with suitable mechanical strength and appropriate biocompatibility for optimum function involves a multidisciplinary approach. The analysis of the molecular constituents of soft tissue and their mutual interaction are usually the province of the biochemist and histologist. The gross behaviour of tissue when subjected to load or pressure is often studied by a bioengineer or material scientist. If quantification of the observed behaviour is required then the language of mathematics must be involved. The emphasis of the work presented here will be on the macroscopic properties of the tissue. However, an understanding of the microstructure is also required if the mathematical models, which are developed to describe the material behaviour, are to be appreciated fully.

Although as early as 1847, Wertheim suggested that, for tendon, stress might be related exponentially to strain, the study of living tissues by modern engineering techniques only developed around 1960. One of the first tissues to be investigated was skin. This latter work arose from an attempt to provide the plastic surgeon with quantitative information which would eliminate some of the trial and error involved in reconstructive surgery [1].

The standard procedure for assessing a material's static tensile properties involves the application of uniaxial loading. When a rectangular metal strip is subjected to a uniaxial load it is assumed that the induced stress depends only on the current deformation. For metals the deformation gradient is extremely small and the strain

0022–2461/85 $03.00 + .12

measure can be considered as infinitesimal. Thus the stress can be represented, to a good approximation, by a linear function of the infinitesimal or linear strain. As a consequence the observed variation of stress with infinitesimal strain lies on a straight line over a wide range of loads. The slope of the stress–strain curve (Young's modulus, E) provides a measure of the uniaxial extensibility of the material. The ratio of the contraction in the width and the extension of the length of the test specimen (Poisson's ratio) is related to the volume changes in the specimen which can arise during uniaxial loading. For infinitesimal strains a measure of the volume change is provided by the cubical dilatation. The ratio of the hydrostatic pressure (one third of the sum of the normal stresses) and the cubical dilatation defines the bulk modulus, K. These three parameters which characterize the elastic model of a material are related by the equation

$$K = E/3(1-2\gamma) \qquad (1)$$

It also follows that if $K \gg E$ then $\gamma \simeq \frac{1}{2}$ and the material is said to be incompressible.

When skin was tested, by these engineering methods, it was discovered that this living tissue deviated from the idealized Hookean elastic model in a number of ways.

1. The tissue exhibited a highly non-linear relationship between stress and the extension ratio in the direction of load [2].

2. The material could be extended by up to 30% for relatively small loads, so that the strain measure was no longer infinitesimal.

3. When skin was loaded suddenly and then maintained at a constant extension the stress was gradually relaxed over a period of time [3].

4. Mechanical energy was dissipated during the loading and unloading of the tissue since the phenomenon of hysteresis was observed. Also irreversible plastic deformation and strain hardening was observed during repeated cyclic testing [4].

The problem of characterizing a material that displayed a non-linear relationship between stress and extension ratio had been tackled earlier by workers in rubber and leather technology. To analyse the observed response of vulcanized rubber to load, the concept of a potential energy function which depended only on the current state of non-linear strain was used [5]. This approach models the material as an idealized non-linear elastic solid and neglects any energy losses or response delays caused by viscous dissipation. In general the strain energy function depends on the individual components of the matrix representation of the strain tensor. However, when the material is isotropic (no preferred mechanical properties in the unstrained state) it can be shown that the strain energy function depends only on the strain invariants of the strain tensor [5].

Mechanical testing of vulcanized rubber [5] suggested that these materials were isotropic. Furthermore although small changes in volume (expansions) were observed during uniaxial loading [6] rubber has usually been considered as an incompressible material. The assumptions of isotropy and incompressibility allowed the construction of relatively simple elastic constitutive equations, in terms of a strain energy function, which adequately described the mechanical behaviour of vulcanized rubber in a number of different experimental situations [5].

The majority of workers who first studied the response of skin to uniaxial loading fitted their experimental results by means of a power low relation or an exponential function [7]. Although this approach allows a quantitative comparison to be made between different tissues, between the same tissue at a different age and between chemical treatments of the same tissue it is limited in its application. In the first place the underlying physics which determines the observed response to load is lost by simple curve fitting. Secondly extrapolation to non-uniaxial problems is virtually impossible.

Recognizing the inadequacy of soft tissue characterization in terms of Young's modulus, Fung [8] introduced a strain energy function, W, which he assumed depended only on the extension ratio, λ, in the direction of load. Fung assumed a linear relation existed between stress, σ, and the slope $d\sigma/d\lambda$ of the stress–strain curve. By solving the equation $d\sigma/d\lambda = k\sigma$, not surprisingly, he showed the stress was an exponential function of λ. When the slope of the stress–strain curve was expressed as a quadratic function of stress the experimental points could be fitted by a four-parameter non-linear function characterized by the presence of an exponential function. Since this characteristic exponential factor is absent in the strain energy functions used to describe vulcanized rubbers, Fung concluded that rabbit mesentery is entirely different to vulcanized rubber.

Experiments performed by Carew *et al.* [9] on the canine thoracic aorta have purported to show

that the arterial wall is incompressible, to a good approximation. This work has been quoted by Lanir and Fung [3] as evidence that skin is incompressible in the physiological stress range. However, the fact that Carew *et al.* [9] based their conclusions on the comparison of engineering parameters, that have no relevance in the non-linear finite deformation behaviour of biological tissue, suggests that the assumption of incompressibility should be viewed with caution.

Lanir and Fung [3] used the incompressibility assumption to calculate the contraction ratio, λ_3, in the vertical direction perpendicular to the plane of the tissue subjected to uniaxial load. They measured, λ_1, the extension ratio in the direction of load and the contraction ratio, λ_2, in the plane of the tissue. From the measured values of λ_1, and λ_2 and the assumption of incompressibility

$$\lambda_3 = 1/\lambda_1\lambda_2. \qquad (2)$$

The computed value of λ_3 was not equal to the measured value of λ_2 at any experimental point during uniaxial tension tests. A difference between λ_2 and λ_3 for a specimen under uniaxial load implies that the material is anisotropic. If, however, the material is compressible, Equation 2 will be invalid and λ_3 cannot be computed, but must be measured, to compare with the measured value of λ_2.

Experiments performed by Patel [10] on arterial canine segments have been quoted as evidence that arteries are anisotropic. These experiments have been interpreted in terms of linear elastic constitutive equations, albeit with quite general elastic symmetries. If stress is related non-linearly to the current strain for biological tissue any interpretation based on linear theories must be treated with suspicion. However, Vaishnav *et al.* [11] have then used the incremental response of canine aorta to pressure to evaluate the initial incremental elastic moduli associated with radial, axial and azimuthal directions. Differences in these moduli have been attributed to the anisotropic properties of the tissue. Alternatively, Tickner and Sacks [12] have based the static elastic behaviour of blood vessels on an isotropic compressible theory of non-linear elasticity.

In the last ten years there has been a significant increase [13] in the use of leaflet-type heart valve substitutes. These bioprostheses are generally of two types, namely (i) chemically treated and frame mounted porcine valves and (ii) chemically treated bovine pericardium pressure formed and mounted on a frame to produce a three-leaflet configuration. In both cases the chemical treatment involves the use of appropriately buffered glutaraldehyde. This process has been shown to provide appropriate antigenicity of the finished valve whilst also increasing the number of collagen cross-links, and thus enhancing the mechanical strength of the tissue.

A number of studies by Broom [14–17] have investigated the morphological and mechanical effects of glutaraldehyde fixation on valve-leaflet tissue. Glutaraldehyde fixation introduces a large number of stable cross-links between the amino acid groups of the polypeptide chains of collagen and supplements the cross-links which occur naturally in the untreated tissue [17]. The alteration in mechanical properties of the tissue through such fixation techniques has been portrayed by a different mechanical response to uniaxial load [17]. There has been no attempt in these studies to interpret the experimental observations by parametric characterization of the leaflet tissue.

However, Rabkin and Hsu [18] have proposed a number of mathematical and mechanical models to describe the relationship between stress and strain in untreated pericardium. On the basis of goodness of fit to observed data the stress was expressed as an exponential function of extension ratio (referred to as strain) which depended on two material parameters. As in earlier descriptions of other tissues the modelling procedure was empirically based and lacked physical derivation.

The study presented here attempts to clarify both the terminology and the analytical inconsistences which have arisen in earlier studies of soft tissue behaviour. A brief discussion of the microstructure of pericardium is followed by the construction of a continuum approximation of the tissue. A comparison of the characteristic time in the problem being investigated and the tissue relaxation time is used to invoke an elastic constitutive equation for the glutaraldehyde fixed pericardium tissue. Reference is made to the molecular constitution of the material when deciding on the most appropriate form of the elastic strain energy function for this constitutive equation. The physical concepts of isotropy, compressibility and homogeneity are defined within the framework of non-linear elasticity theory before a specific isotropic, compressible elastic

model of the tissue is constructed. The authenticity of the model is tested by its ability to *predict* the observed functional relationship between induced stress and the axial extension ratio in an uniaxial load test. Mathematical analysis is used to determine the slope of the stress–extension ratio curve in the limit of zero load. In this way the mechanical response to load, in the unstrained state, in different uniaxial directions can be computed from the experimental observations. Finally, the possible relevance of the material characterization presented here is discussed with respect to other soft biological tissue.

2. Theoretical concepts

2.1. The structure of bovine pericardium

The pericardium in mammals consists of two parts: an outer, fibrous pericardium and an inner, double layered sac called the serous pericardium. It is the combined outer layer of the serous pericardium and the fibrous pericardium which is used to construct bioprosthetic heart valve leaflets. This soft collagenous tissue consists predominantly of collagen, elastin, ground substance and water. Collagen is the polypeptide chain which when organized into fibres is thought to dominate the structural integrity and gross mechanical behaviour of the tissue. Elastin is a globular rather than helical protein. Four lysine-derived units join to form the four-pronged desmosine link that ties four elastin polypeptide chains together. The ground substance consists of mucopolysaccharide, glycoproteins and soluble proteins and accounts for less than 1% of the total tissue weight. Bovine pericardium in its natural state consists of 76% by weight of water [33]. Almost all of this water is unbound.

TABLE I Construction of the largest collagen unit, the collagen fibril

Basic unit – "the α chain"	left-hand helix, polypeptide molecular chain
3 α chains – tropocollagen molecule	right-hand superhelix, rod like, length 290 nm, diameter 1.4 nm. Cross-links in the terminals
5 staggered tropocollagen molecules – "pentafibril"	Extensive intermolecular cross-links and inter-fibrillar cross-links
Aggregation – of pentafibrils	Collagen fibril, 100 nm diameter

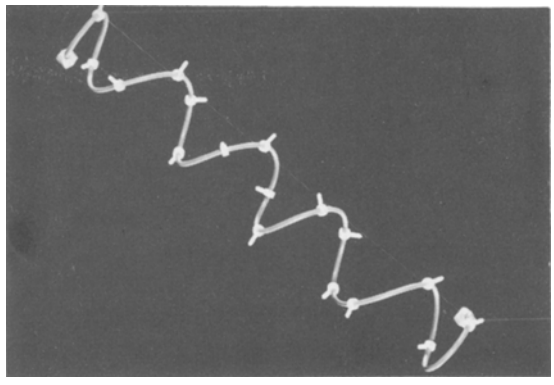

Figure 1 A model of a portion of the left hand helical collagen polypeptide α chain. The projections perpendicular to the basic helix represent the individual amino acid side chains. There are usually 1050 amino acids in one collagen helix.

Since chemical treatments introduced to provide biological stability and enhance gross mechanical strength are directed specifically at the collagen molecule, the construction of the largest collagen unit, the collagen fibril, is summarized in Table I. Models of the polypeptide α chain, the tropocollagen molecule and the pentafibril are displayed in Figs. 1 to 3.

Naturally occurring intra-molecular cross-links are found in the amino terminals (N terminals) of the triple helix. Interfibrillar cross-links arise from a reaction between lysine derived aldehyde and lysine or hydroxylysine.

Glutaraldehyde is a bifunctional aldehyde which is able to cross-link two molecules of

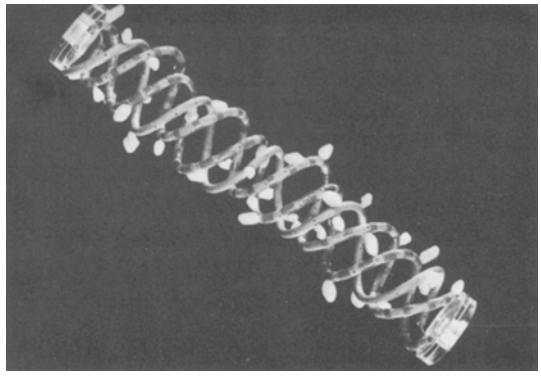

Figure 2 A model of a portion of the right-hand superhelix, the tropocollagen molecule. The unit is constructed from three left-hand α chains. These chains are represented by the helices with one, two and no circumferential bands. The attached "beads" again represent the amino acid side chains.

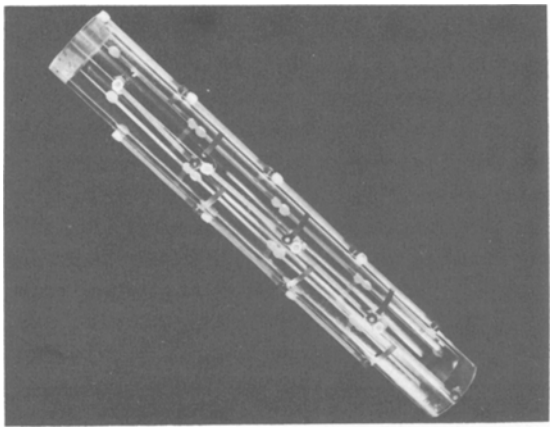

Figure 3 A model of a protion of the collagen pentafibril. The rods represent a tropocollagen molecule. The dark circle represents the amino (N) terminal and the light circle represents the carboxyl (C) terminal of the tropocollagen molecule. It can be seen that the N terminals trace out a helix around the cylindrical structure. The dark bands represent potential sites of natural and artificially induced intra-molecular cross-links.

collagen by forming covalent bonds. Its molecular size appears to be particularly suitable for bridging the gaps between the amino terminals, usually through the lysine or hydroxylysine residues, of collagen polypeptide chains. As a consequence glutaraldehyde treatment of natural bovine pericardium induces collagen molecular cross-linking above that found in the natural state. This in turn alters the gross mechanical properties of the tissue when tested under load [17]. There is virtually no change in the total water content of the tissue after glutaraldehyde fixation [33].

The inherent molecular complexity of the tissue suggests that a quantitative microstructural theory of the response of the pericardium to load would lead to mathematical intractability if all the molecular forces are realistically considered. For this reason a continuum physics approximation of the real tissue behaviour is usually invoked when quantifying the mechanical properties of both the natural and glutaraldehyde treated pericardium. Only glutaraldehyde fixed material will be considered here.

2.2. The continuum physics approximation

In order to develop a mathematical theory which describes the macroscopic behaviour of materials the microscopic structure is usually disregarded [19–21]. The material is considered to be continuously distributed throughout some region of space. At any instant of time, every point in the spatial region is occupied by a particle, known as the material particle. A material body, in this study a volume of pericardium, is idealized as a set of material particles such that, at each instant of time, t, each particle of the set is assigned to a unique point of a region R in three-dimensional Euclidean space. It is assumed that each point in R is occupied by just one particle.

In reality any measuring device or "observer" usually averages the material microscopic structure over a small finite spatial volume and over a small finite time interval. If the characteristic length associated with the spatial volume is small compared with the smallest characteristic macroscopic length, as in the problem under consideration, then the spatial volume is considered to be a point, the material point, on the macroscopic length scale. For example, the typical thickness of the calf pericardium tissue used in this study, is of the order of 0.3 mm. If this thickness is divided into 100 (say) equal parts to give a characteristic length scale of 3 μm, then a sphere with a diameter 3 μm can be considered as a material point on the macroscopic scale. The molecular structure of the tissue is averaged over this volume, at an instant, to obtain the material point macroscopic characteristics of the tissue.

It has been shown elsewhere (see Trowbridge [22]) that the above concept should also be applied to time, since the time resolution as well as the space resolution of an observer creates the illusion of a continuously distributed material on which the mathematical idealization is based. However, the inter-molecular forces in those materials which display solid-like characteristics are considered to be much greater than the forces experienced in those materials with fluid-like characteristics and as a consequence it is assumed that there will be relatively little change with time in the relative positions of the constituent molecules in soft biological tissue such as skin, tendon or pericardium.

The importance of these concepts becomes apparent when it is realized that the average properties of *all* the molecules, which includes the numerous cross-linkage bonds in collagen and elastin, in the "small" material volume at an instant, provide the continuum point properties in the mathematical description of soft biological tissue. The fibrous nature of the collagen constituent can often be observed in soft tissue. The inter-

molecular cross-links cannot. A substantial number of collagen fibres (diameter 100 nm) can exist in a "small" sphere of diameter 3 μm. The continuum approximation "smoothes out" the microstructural complexity of the tissue and the commonly held concept of collagen fibres in a background matrix is no longer appropriate with this (3 μm say) continuum length scale.

2.3. What is a suitable constitutive equation?

In order to describe the behaviour of materials mathematically, some idealization of the real material is usually necessary. In the classical linearized theory of elasticity, the stress in a sheared body is taken to be proportional to the amount of shear. The Navier–Stokes theory of viscous fluids takes the shearing stress to be proportional to the rate of shear. In most materials, under appropriate circumstances, effects of both elasticity and viscosity are noticeable. As a consequence, the idealization which best describes the material depends strongly on the *circumstances* under which the material is being investigated [23]. For example, the "therapeutic putty" which is used for physiotherapeutic purposes, bounces like an elastic ball but flows like a fluid when left on the laboratory bench. The same material would be idealized as an elastic material in the former "short" time scale collision problem and yet fluid-like properties would be attributed to it in the latter "long" time scale problem. The same problems of idealization arise in modelling soft biological tissue. The hysteresis loop that Lanir and Fung [3] observed during the initial loading and unloading of tissue in an uniaxial test indicates that energy is dissipated during stretching of the tissue. Moreover, stress relaxation of soft tissue occurs if observations are made over a sufficiently long time scale. For example, the stress relaxation in rabbit skin is less than 5% in 1 sec but can be as much as 25% in 10 min [3].

However, the time scale of deformation (loading and unloading) for a heart valve leaflet is approximately 1 sec, since the valve opens and closes about sixty times per minute. Furthermore, the long term objective of mechanical characterization of glutaraldehyde fixed pericardium is the analysis of operational stresses in the prosthetic heart valve leaflet, in order to determine optimum designs. As a consequence if the relaxation time of the fixed tissue is long compared with 1 sec and the observed stress, during uniaxial loading, is relatively independent of strain rate then the circumstances under which the valve leaflet operates would suggest an elastic idealization of the real material, even though the tissue may exhibit viscoelastic properties in different circumstances.

2.4. The concept of strain energy, elastic symmetry and isotropy

A consideration of the mechanical energy equation suggests that a finite elastic material inherently possesses potential energy when it is loaded [21]. It is this potential for doing work in the stressed state which produces the elliptical wounds, observed by Langer [24], when skin is incised. The inherent potential energy depends on the elastic deformation of the material and is usually considered to be a mathematical function of the measure of finite strain. In general, for an elastic material which has no apparent elastic symmetries, the strain energy function, W, can be written as

$$W = W(B_{11}, B_{12}, B_{13}, B_{22}, B_{23}, B_{33}), \quad (3)$$

where B_{ij}, $i, j = 1, 2, 3$, are the components of the left Cauchy–Green strain tensor referred to a rectangular Cartesian coordinate system Ox_1, x_2, x_3 [21].

If the elastic material possesses no preferential directional properties *in the unstressed state* then the strain energy will have the same functional form under any rigid body rotation of the rectangular Cartesian axes. It can be shown [25] that invariance of the functional form of W is possible if, and only if,

$$W = W(I_1, I_2, I_3),$$

where I_1, I_2, I_3 are the three strain invariants (invariant under the rotation of coordinate axes) derived from the scalar characteristic equation which is related to the left Cauchy–Green strain matrix [21].

An elastic material whose inherent potential energy has this functional form is said to be isotropic. Materials with specific directional properties will only have elastic symmetries about planes and directions determined by these properties. They are called anisotropic. Evidence of anisotropy is provided experimentally by a different initial mechanical response to load in different material directions.

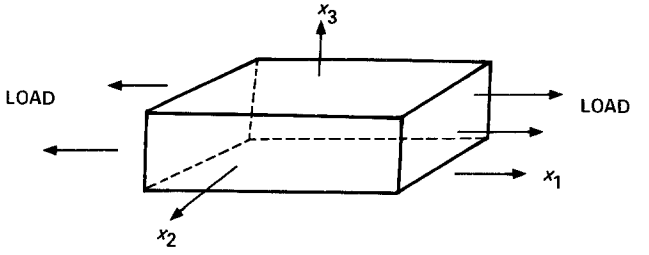

Figure 4 A schematic representation of the uniaxial loading of a rectangular block of glutaraldehyde-fixed bovine pericardium. The rectangular cartesian coordinate system has the x_1-axis in the direction of load and the x_2-, x_3-axes perpendicular to the load. The strain invariants, I_1, I_2, I_3, can be expressed in terms of the extension ratio, λ_1 and the contraction ratios λ_2, λ_3, when referred to this specific coordinate system.

$$I_1 = \lambda_1^2 + \lambda_2^2 + \lambda_3^2$$

$$I_2 = \lambda_1^2\,\lambda_2^2 + \lambda_2^2\,\lambda_3^2 + \lambda_3^2\,\lambda_1^2$$

$$I_3 = \lambda_1^2\,\lambda_2^2\,\lambda_3^2 = (V/V_0)^2$$

2.5. Compressibility

The test for compressibility that is usually employed in infinitesimal elasticity compares the bulk modulus and the Young's modulus of the material. As explained in Section 1 the bulk modulus is obtained from the ratio of the hydrostatic pressure and the dilatation. The dilatation is a measure of volume change in infinitesimal elasticity theory [26]. In uniaxial load tests the only non-zero stress, σ, is that in the direction of load. As a consequence the hydrostatic pressure is $\sigma/3$. The dilatation is given by the sum of the infinitesimal strains $(e_{11} + e_{22} + e_{33})$. It can be shown that the physical meaning of the infinitesimal normal strain component e_{11} is the increase in length divided by the original length and e_{22} and e_{33} represent the contraction in width and thickness divided by the original width and thickness, respectively [21]. Unfortunately, biological tissue neither obeys Hooke's law nor are the strains infinitesimal. The strain measure is non-linear and finite and the normal strain components no longer physically represent the change in length divided by the original length as above. Indeed it can be shown [21], that the left Cauchy–Green finite elastic normal strain components can be written as

$$B_{11} = (\lambda_1^2 - 1), B_{22} = (\lambda_2^2 - 1), B_{33} = (\lambda_3^2 - 1), \tag{5}$$

where λ_1, λ_2, λ_3 are the principal extension and contraction ratios, respectively [21]. For this reason the dilatation no longer provides a measure of volume changes, and the ratio of the volume after the deformation, V, to that before the deformation, V_0, is given by

$$(I_3)^{1/2} = \lambda_1\lambda_2\lambda_3 = V/V_0. \tag{6}$$

If the extension under load is balanced by suitable contraction in the width and thickness then I_3 remains constant and equal to unity and the volume is unchanged during the deformation. The material is then incompressible. If I_3, and hence V, change with load the material is classified as compressible.

2.6. The homogeneous deformation of an isotropic compressible elastic material subjected to uniaxial load

If a rectangular block of isotropic compressible elastic material is subjected to a uniaxial load, F, then referred to the rectangular Cartesian coordinate system described in Fig. 4, the stress components in the directions Ox_1, Ox_2, Ox_3 are given by

$$\frac{F}{A} = \sigma = \frac{2}{\lambda_1}\left[\lambda_1^2\frac{\partial W}{\partial I_1} + \left(I_2 - \frac{I_3}{\lambda_1^2}\right)\frac{\partial W}{\partial I_2} + I_3\frac{\partial W}{\partial I_3}\right] \tag{7}$$

$$0 = \frac{2}{\lambda_2}\left[\lambda_2^2\frac{\partial W}{\partial I_1} + \left(I_2 - \frac{I_3}{\lambda_2^2}\right)\frac{\partial W}{\partial I_2} + I_3\frac{\partial W}{\partial I_3}\right] \tag{8}$$

$$0 = \frac{2}{\lambda_3}\left[\lambda_3^2\frac{\partial W}{\partial I_1} + \left(I_2 - \frac{I_3}{\lambda_3^2}\right)\frac{\partial W}{\partial I_2} + I_3\frac{\partial W}{\partial I_3}\right], \tag{9}$$

where $W = W(I_1, I_2, I_3)$ is a measure of the strain energy induced by the load F, and A is the cross-sectional area of the block, perpendicular to the direction Ox_1, before the deformation.

If the material is isotropic, then $\lambda_2 = \lambda_3$ and Equations 8 and 9 are identical.

Elimination of $\partial W/\partial I_3$ between Equations 7

and 8 yields

$$D = \frac{\sigma}{2(\lambda_1 - \lambda_2^2/\lambda_1)} = \frac{\partial W}{\partial I_1} + \lambda_2^2 \frac{\partial W}{\partial I_2}. \quad (10)$$

A Taylor series expansion of $W(I_1, I_2, I_3)$ about the equilibrium position $I_1 = 3$, $I_2 = 3$, $I_3 = 1$ yields

$$W(I_1, I_2, I_3) = W(3, 3, 1) + \frac{\partial W_E}{\partial I_1}(I_1 - 3) + \frac{\partial W_E}{\partial I_2}(I_2 - 3) + \text{terms in } I_3 \text{ and higher order terms.} \quad (11)$$

The partial derivatives $\partial W_E/\partial I_1$, $\partial W_E/\partial I_2$ are evaluated at the equilibrium position and are constants. Setting

$$\frac{\partial W_E}{\partial I_1} = c_1, \frac{\partial W_E}{\partial I_2} = c_2 \quad (12)$$

gives the stored potential energy, to the first order, in I_1 and I_2, induced by uniaxial load, as

$$W(I_1, I_2, I_3) = c_1(I_1 - 3) + c_2(I_2 - 3) + \text{terms containing } I_3, \quad (13)$$

since it is assumed that the potential for doing work in the relaxed state is zero.

The variation of the potential energy with I_3 (and consequently volume, since $I_3 = (V/V_0)^2$) is given by Equation 8, through the partial derivative $\partial W/\partial I_3$. Using this formulation, Equations 10 and 13 imply that to a first approximation

$$D = c_1 + \lambda_2^2 c_2, \quad (14)$$

which indicates that D is a linear function of λ_2^2.

Consideration of the ratio

$$e_{33}/e_{11} = e_{22}/e_{11} = \text{constant (Poisson's ratio)}$$

which applies to infinitesimal elasticity theory, for an isotropic material, suggests that it is simply a linear first order approximation to the more general relation

$$\frac{B_{33}}{B_{11}} = \frac{B_{22}}{B_{11}} = f(B_{11}), \quad (15)$$

where f is an arbitrary function of the left Cauchy–Green finite normal strain, B_{11}, in the direction of load. Physically, this mathematical statement suggests that contraction in the two directions perpendicular to the load is dependent on the uniaxial extension induced by the load. Written in terms of the principal extension and contraction ratios, λ_1, λ_2 and λ_3, Equation 15 becomes

$$\frac{\lambda_2^2 - 1}{\lambda_1^2 - 1} = f(\lambda_1^2 - 1). \quad (16)$$

Expanding in a Taylor series about the equilibrium state $\lambda_1 = 1, \lambda_2 = 1, \lambda_3 = 1$, yields to second order

$$\frac{\lambda_2^2 - 1}{\lambda_1^2 - 1} = k + m(\lambda_1^2 - 1) + n(\lambda_1^2 - 1)^2. \quad (17)$$

When λ_2^2 has been determined as a polynomial, $P(\lambda_1)$, from Equation 17, then Equation 14 *predicts* the variation of stress with principal extension ratio λ_1, namely

$$\sigma = 2(\lambda_1 - P(\lambda_1)/\lambda_1)(c_1 + P(\lambda_1)c_2) \quad (18)$$

where

$$P(\lambda_1) = 1 + k(\lambda_1^2 - 1) + m(\lambda_1^2 - 1)^2 + n(\lambda_1^2 - 1)^3. \quad (19)$$

Equation 18 provides a non-linear relation between σ and λ_1, the slope of which varies with the extension ratio λ_1, induced by the load.

The slope of the stress–extension ratio curve at the origin provides a measure of the mechanical properties (i.e. the response to load) in the relaxed state of the material.

Differentiating Equation 18 with respect to λ_1 and letting $\lambda_1 \to 1$ gives

$$\frac{d\sigma}{d\lambda_1} = 4(1 - k)(c_1 + c_2). \quad (20)$$

3. Materials and methods

3.1. Preparation of standard glutaraldehyde-treated pericardium

Pericardium taken from 16 to 20 week-old calves was transported in ice-cold isotonic saline (0.9% NaCl) from the abattoir. The pericardium was stripped to remove any fat and then placed loosely on 150 or 100 mm diameter embroidery frames. The tissue was then immersed in 0.2% solution of glutaraldehyde (BDH Chemicals Ltd) buffered to pH 7.4 in 0.2 M phosphate buffer (Sorensen). The pericardium was fixed for 7 days before testing.

3.2. Tissue selection and test specimen preparation

Homogeneous strips of pericardium for testing were obtained by visual appearance. Regions which varied substantially in thickness or con-

tained tendon attachments were eliminated from the test procedure. A parallel bladed cutter with blades 11 mm apart was used to stamp out strips 79 mm long. These were trimmed to lengths of approximately 60 mm. Tissue thickness was measured with a Mitusoye thickness gauge to within an accuracy of ± 0.02 mm. Small perspex blocks (12 mm x 17 mm x 3 mm), with a hole for screw attachment to the test rig, were glued on to the ends of the tissue strip with cyano-acrylate adhesive. The approximate lengths of free tissue between the blocks was 40 mm. Two short lengths (6 to 7 mm) of black 4/0 silk sutures were glued at their mid-points to the middle of the tissue strip, close to and parallel to the longitudinal edges of the specimen by cyano-acrylate adhesive.

3.3. Uniaxial load test apparatus

A servo-motor driven assembly was used to load the tissue specimen. The applied force was measured by a Statham force transducer. The changes in tissue length and width between the silk sutures were measured by a displacement transducer and video extensometer, respectively. The servo-motor possessed the facility for both a single load/unload test and cyclic loading. A three-channel calibrated pen recorder was used for force, length and width output.

3.3.1. Uniaxial load test procedure

The prepared specimen was attached to the rig, the position of the moving clamp was adjusted to obtain a fully relaxed specimen, without stretch or sag. The distance between the edges of the perspex grips, where the tissue was attached, was measured with a steel rule to an accuracy of 0.5 mm. The width of tissue between the sutures was measured using the video extensometer. The pens of the recorder were zeroed. The specimen was kept moist throughout the test by immersion in a bath of isotonic (0.9%) saline. A recirculating peristaltic pump and overflow guttering maintained a constant fluid level in the bath. All tests were performed at room temperature.

The test system was set to give maximum load of 3 N. Beyond this level slippage in the perspex grips was observed. Single tests and cyclic tests (eight cycles) at different strain rates were undertaken. The average error ($n = 10$), at maximum load, between using the extensometer and the displacement transducer for axial displacement measurement was less than 0.6% in the extension ratio.

3.3.2. Stress–relaxation test

The procedure for specimen preparation and test were those described above. The load was set at 3 N. The step load facility available on the servo-motor was utilized to impulsively load the tissue. At maximum load the tissue was maintained at the same extension (verified by the displacement transducer) and the relaxation in stress was recorded for 1000 sec by the force transducer.

3.4. Comparison of the mechanical response to load from position to position and sac to sac

Five pericardial sacs were fixed with glutaraldehyde by the method described above. After treatment six regions, emanating radially from the sac apex, were marked out. A single strip was cut from each region so that the longitudinal axis of the strip lay along the radius. Wherever possible the specimen was removed from the identical position in the region for each sac. Eight further strips were cut at random from two other sacs, no preference being given to position or direction other than to satisfy the criterion of thickness and tissue uniformity described earlier.

4. Results

4.1. Stress relaxation

Fully conditioned (cyclically loaded and unloaded eight times) tissue was loaded impulsively to 3 N and the extension induced was then maintained. Fig. 5 shows a typical variation of stress with time. It can be seen that the stress varies linearly with $\log_e$(time). The relaxation time is usually defined as the time required for the stress to fall to $0.368(e^{-1})$ of its original value [26]. The relaxation time of this specific specimen would be greater than 10^5 yr. All specimens tested had relaxation times of the order of many years, whether they were conditioned or the stress was allowed to relax after the first elongation. However, this definition relies on a relaxation function

$$G(t) = \exp(-t/\tau),$$

where τ is the relaxation time, derived from a linear viscoelastic Maxwell model. The relaxation function for glutaraldehyde treated pericardium is

$$H(t) = A \log_e t + B,$$

where A and B are time independent. This equation can be rewritten as

$$H(t) = A \log_e(t/\tau),$$

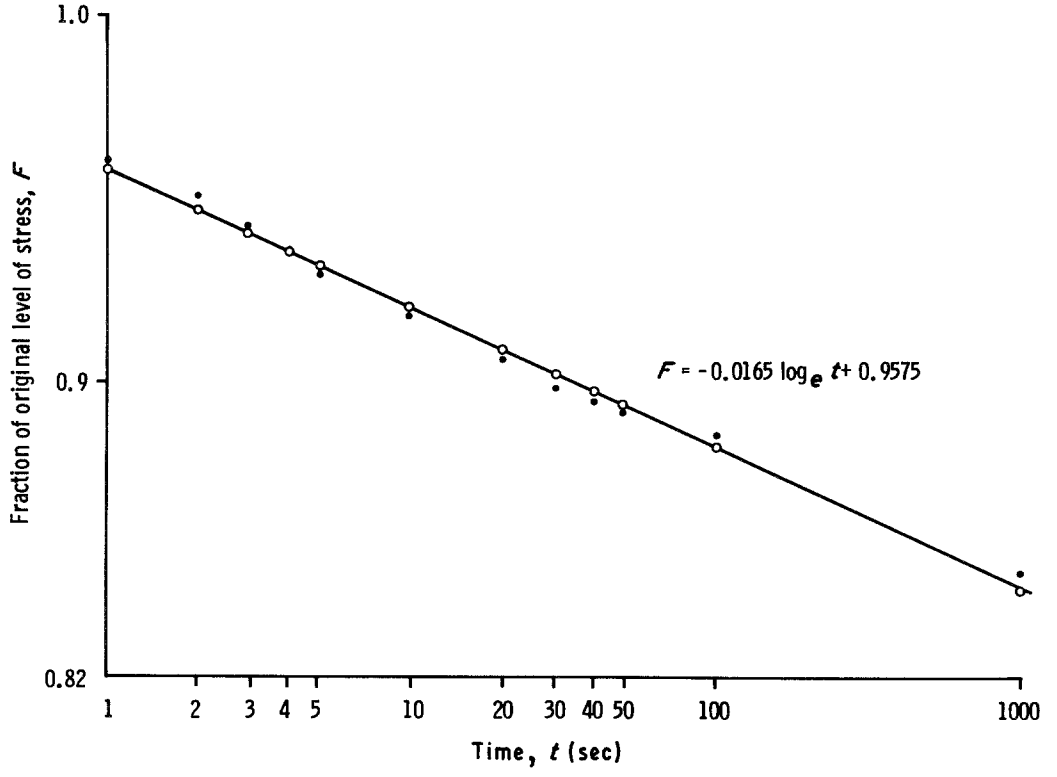

Figure 5 The relaxation of stress with time when a specimen of glutaraldehyde-fixed pericardium is held at a fixed extension. The logarithmic decay of stress with time displayed here was typical of all specimens tested.

where $\tau = \exp(-B/A)$ is defined as the relaxation time. A logarithmic relaxation of stress has been reported for other collageneous tissues [27]. With this definition, the relaxation time is the time it takes for a specimen to become stress free. This formulation again gives a relaxation time greater than 10^5 yr.

4.2. Hysteresis and energy dissipation

The effect of conditioning by cyclic loading is shown in Fig. 6. It can be seen that there is a substantial hysteresis loop indicating energy dissipation, on unloading, with a small amount of permanent deformation. However, after eight cycles the tissue loading and unloading curve is essentially the same and further energy losses are minimal.

4.3. The effects of conditioning on the mechanical properties of the tissue

Figs. 7 to 12 show the quantitative changes in the mechanical properties of the tissue that occur as the tissue is conditioned by cyclic loading at the strain rate of $0.004\,\text{sec}^{-1}$. Fig. 7 shows that the strain ratio $(\lambda_2^2 - 1)/(\lambda_1^2 - 1)$ can be approximated by a first order truncated Taylor series in the normal strain B_{11} $(= \lambda_1^2 - 1)$ (see Equation 17). However, the conditioned material in Fig. 8 requires a further quadratic term in the truncation to fit the observed data.

Fig. 9 shows the variation in volume, V, with the principal extension ratio, λ_1, in both the conditioned and unconditioned material. It can be seen that there is an initial expansion of the material to a maximum volume change of 3% at about 12% extension of the tissue.

Fig. 10 shows the agreement between theory and experiment for the variation of λ_2^2 with λ_1 for five consecutive tests of the conditioned material. The dotted line indicates the expected variation of λ_2^2 with λ_1 if the material were incompressible and isotropic.

Fig. 11 shows the variation of D, the strain energy differential (see Equation 14) with λ_2^2 for the conditioned and unconditioned material. Although the relationship between D and λ_2^2 is linear the predicted stress–extension ratio curves are non-linear. The theory predicts the variation

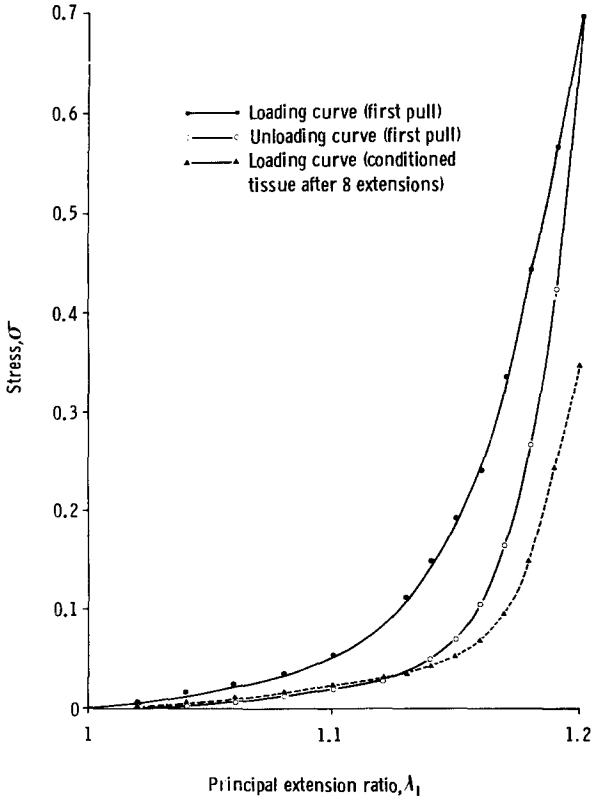

Figure 6 The effects of tissue conditioning by cyclical loading and unloading. The loading curve (•) maximum stress is reduced by 50% after eight cyclical uniaxial extensions of the specimen (▲).

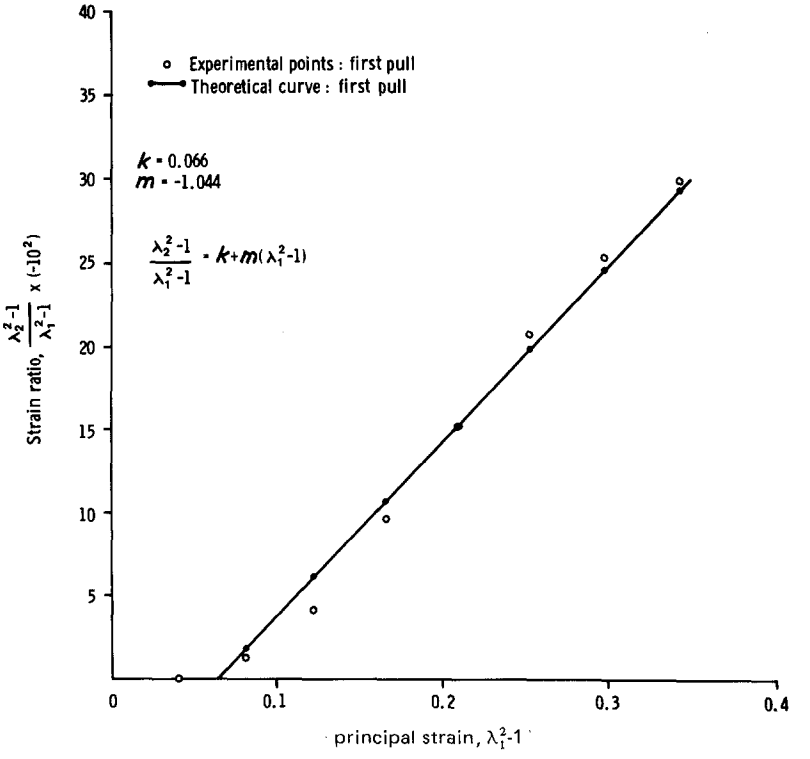

Figure 7 The variation of strain ratio, $B_{22}/B_{11} = (\lambda_2^2 - 1)/(\lambda_1^2 - 1)$, with the strain $B_{11} = \lambda_1^2 - 1$, on the initial loading of the specimen. A linear truncation of the Taylor series expansion about the unstrained state provides a good approximation of the observed variation. The straight line is the least square error best fit. The effective Poisson's ratio for this specimen is $-k = -0.066$.

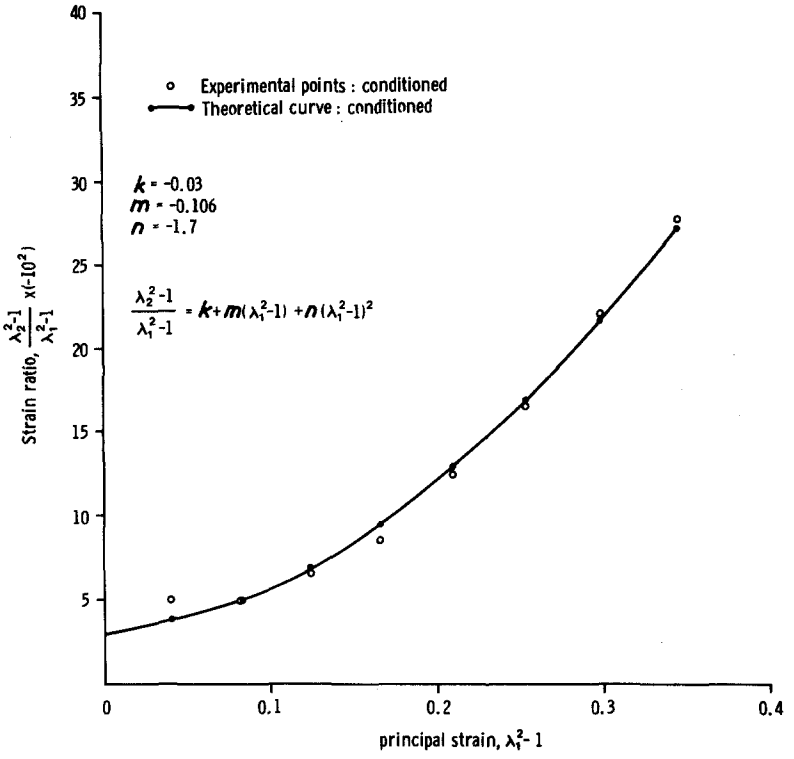

Figure 8 The variation of strain ratio, $B_{22}/B_{11} = (\lambda_2^2 - 1)/(\lambda_1^2 - 1)$ with the strain, $B_{11} = \lambda_1^2 - 1$, for the specimen discussed in Fig. 7 after the specimen has been conditioned by cyclical loading. A quadratic term in the Taylor series expansion of strain about the unstrained state is necessary to describe the observed variation. The effective Poisson's ratio changes from $-k = -0.066$ (Fig. 7) to $-k = +0.03$. Again the theoretical curve is the least square error best fit to the observed data.

of stress accurately over the whole range of deformation, Fig. 12.

4.4. The effect of strain rate on the mechanical properties of the tissue

Figs. 13 to 18 show changes in the parametric values produced by substantially different strain rates for the same conditioned specimen. The low strain rate was set at $0.0008\,\text{sec}^{-1}$ equivalent to an extension rate of $2\,\text{mm min}^{-1}$ for a specimen of length 42 mm, while the high strain rate was set at $0.02\,\text{sec}^{-1}$ which is equivalent to an extension rate of $50\,\text{mm min}^{-1}$. The strain ratio could be satisfied by a quadratic truncation of the Taylor series expansion of the functional variation of normal extensional strain, B_{11}.

Figs. 15 and 16 indicate that the experimental variation of D with λ_2^2 can be fitted by two intersecting straight lines. This suggests that the material undergoes a "phase transition" from one elastic material to a second elastic material as it is being loaded. Experimentally the transition will take place over a range of load. The theoretical transition is at the point of intersection of the two straight lines.

Figs. 17 and 18 show the experimental variation of the stress with the principal extension ratio λ_1, and the stress predicted by the theory. There is excellent agreement between the theoretical predictions and the experimental observations over the whole range of deformation. The slope at the origin predicted from the theory for the high strain rate, $0.02\,\text{sec}^{-1}$, is $0.168\,\text{N mm}^{-2}$ while that obtained from a polygon approximation of the experimental points is $S = 0.15\,\text{N mm}^{-2}$. Similarly the slope at the origin predicted by the theory for the low strain rate, $0.0008\,\text{sec}^{-1}$ is $0.204\,\text{N mm}^{-2}$ which compares favourably with the value $0.20\,\text{N mm}^{-2}$ obtained from the experiment.

Table II shows that the observed stress for a given extension is virtually identical over the whole range of extension. The maximum difference in observed stress for the two strain rates at any point is 4.5% at an extension of 18%.

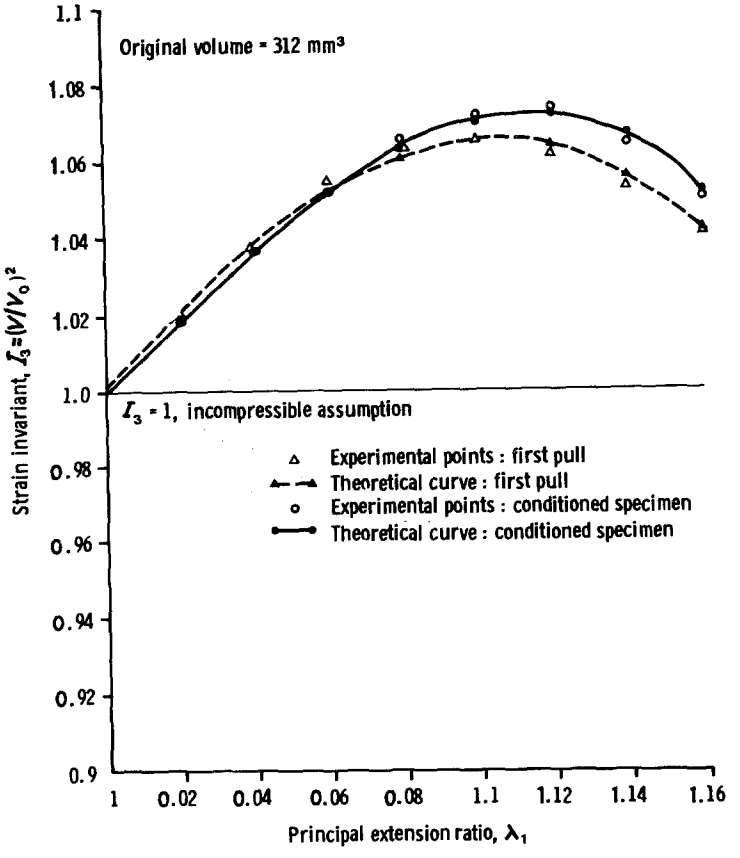

Figure 9 The variation of the square of the volume ratio with extension ratio λ_1. The experimental points were obtained by using the measured values of the extension ratio λ_1, and contraction ratio λ_2 to compute $(V/V_0)^2 = \lambda_1^2 \lambda_2^4$. The theoretical curves were obtained by using the observed values of λ_1, and the values of λ_2 predicted from Fig. 7 and 8 to compute $(V/V_0)^2 = \lambda_1^2 \lambda_2^4$. For an incompressible material $(V/V_0)^2 = 1$ throughout the deformation.

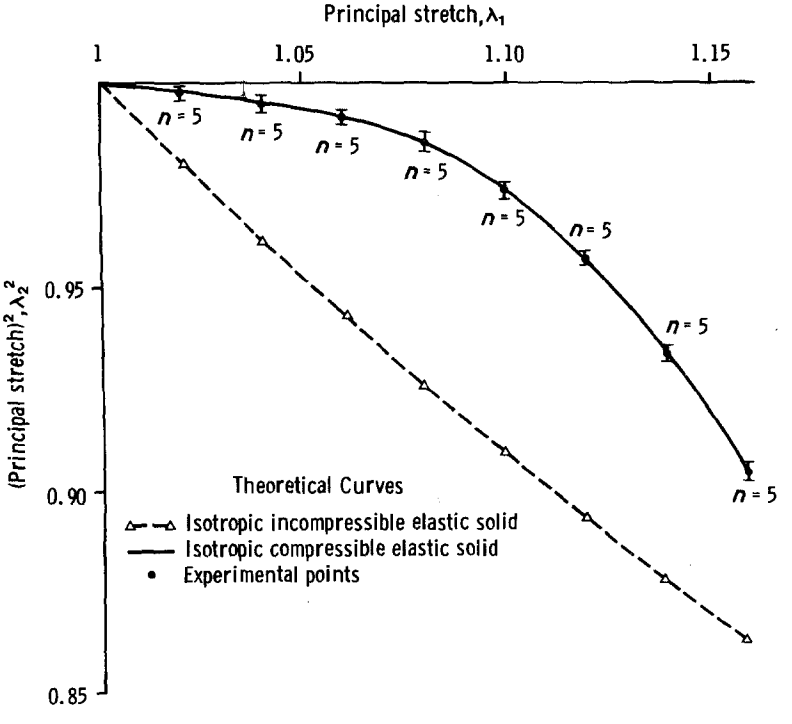

Figure 10 A comparison of the variation of the observed values of λ_2^2 ($n = 5$), after conditioning with λ_1 and the values of λ_2^2 predicted from the truncated Taylor series expansion. The small standard errors indicate that there is little change in the recorded values of λ_2^2 during successive loading of the tissue once it has been conditioned. There is a marked difference between the predicted values of λ_2^2 with a compressible and incompressible model.

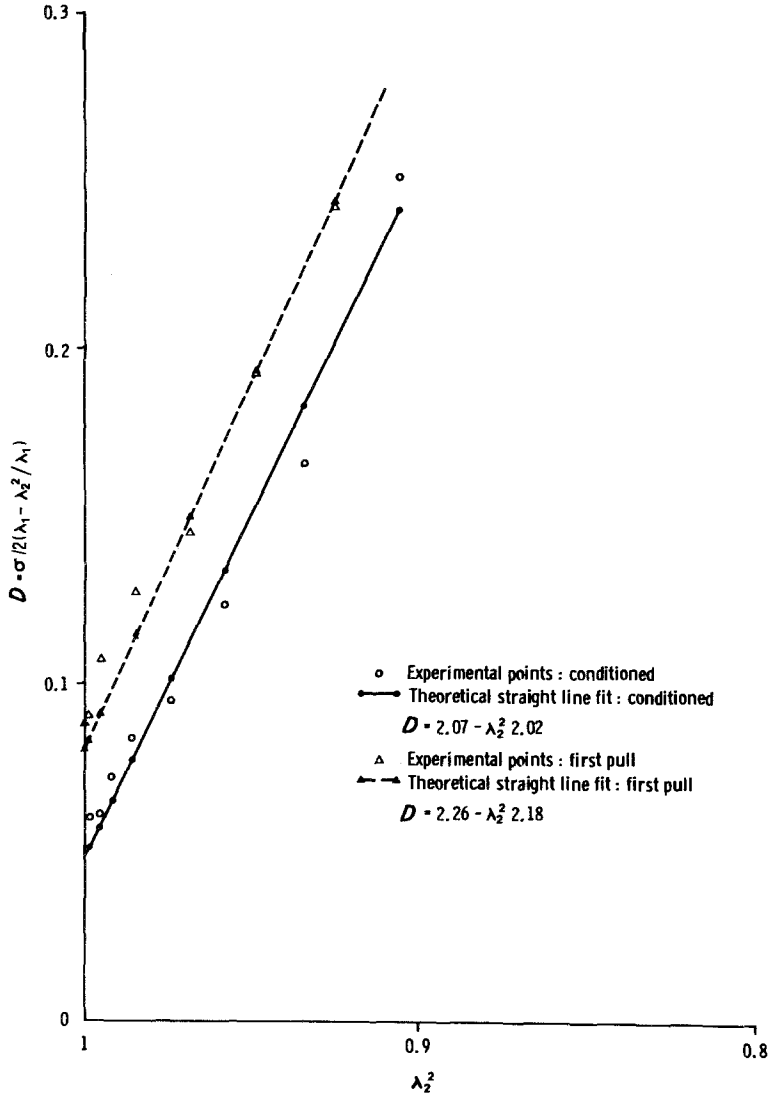

Figure 11 The variation of the strain energy differential, $D = \sigma/2(\lambda_1 - \lambda_2^2/\lambda_1)$ with the square of the contraction ratio, λ_2^2. Both the conditioned and the unconditioned experimental points vary linearly (to a good approximation) with λ_2^2. The theoretical straight lines have been obtained by the least square error best fit to the experimental data.

4.5. Comparison of mechanical properties associated with apparent collagen orientation

Figs. 19 to 22 show the differences in mechanical behaviour that can occur locally in the pericardium. Two pieces of tissue, I_{32} and I_{33}, were cut at right angles to one another in an apparently uniform region of tissue. I_{32} was prepared so that the longitudinal axis appeared to be in the direction of collagen orientation. I_{33} was obtained from a region nearby and prepared so that the collagen fibres appeared to run transversely across the tissue segment.

Fig. 19 shows that in both specimens the functional form of the strain ratio (B_{22}/B_{11}) can be satisfied by a linear truncation of the Taylor series expansion (see Equation 17). There is a substantial difference between the effective "Poisson's ratio" between the two specimens. At small extensions, "Poisson's ratio" (the constant term) is 0.525 for I_{32} while I_{33} takes a value 0.0291. Both specimens undergo a "phase change" on loading as depicted by Figs. 20 and 21. However, these occur at substantially different extensions. Fig. 22 shows that the theoretical transition point for the "stiffer" tissue, I_{32}, occurs at an extension of 10%, while

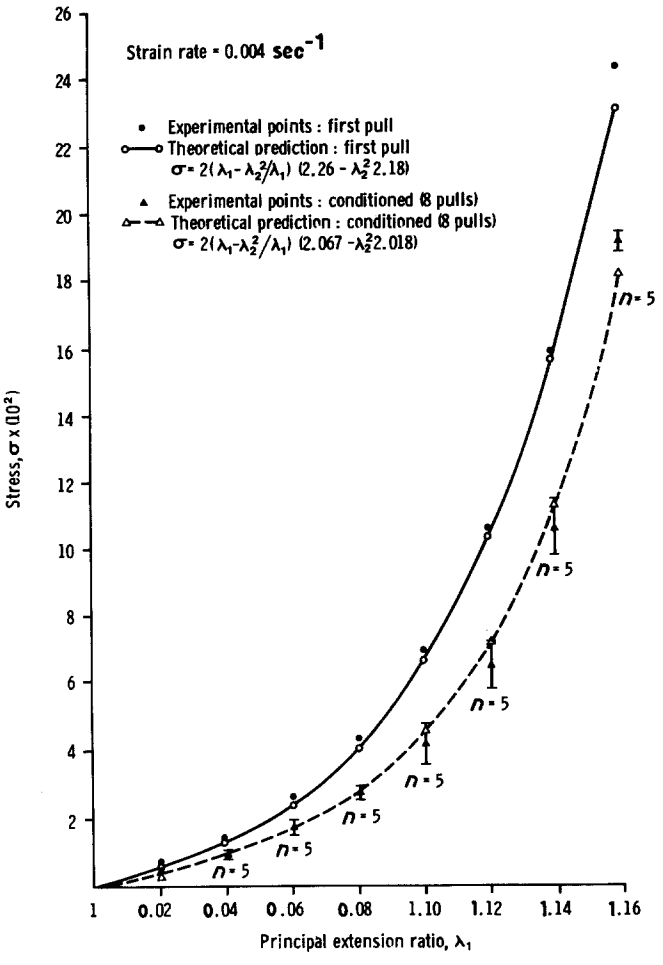

Figure 12 The observed and predicted variation of stress, σ, with principal extension ratio, λ_1, at a strain rate of 0.004 sec^{-1}. The standard error bars indicate the dispersion about the mean of the experimental observations for loading curves ($n = 5$) after conditioning (▲). The curve (Δ----Δ) is the conditioned stress–extension ratio curve predicted from the variation of D with λ_2^2 (Fig. 11) and the variation of λ_2^2 with λ_1 (Fig. 8). The observed variation of stress with extension ratio for the unconditioned specimen (•) indicates a material that is "stiffer" before conditioning than after conditioning. The curve (o——o) is the stress–extension ratio curve predicted from the variation of D with λ_2^2 (Fig. 11) and the variation of λ_2^2 with λ_1 (Fig. 7). Although D varies linearly with λ_2^2 in both the conditioned and unconditioned states of the same specimen, the variation of stress with extension ratio is non-linear.

the specimen I_{33} does not reach its theoretical transition point until an extension of 23% has occurred.

TABLE II The variation of uniaxial stress with extension ratio for two different strain rates

Principal extension ratio, λ_1	Stress (N mm^{-2}) strain rate 0.02 sec^{-1}	Stress (N mm^{-2}) strain rate 0.0008 sec
1.02	0.003	0.004
1.04	0.008	0.009
1.06	0.015	0.015
1.08	0.023	0.023
1.10	0.034	0.035
1.12	0.051	0.050
1.14	0.080	0.078
1.15	0.099	0.097
1.16	0.133	0.133
1.17	0.174	0.177
1.18	0.255	0.267
1.19	0.362	0.349

4.6. The variation of the mechanical properties of the tissue at different positions and from sac to sac

Table III presents the response to load in the unstrained state, measured by the slope at the origin of the stress–extension ratio curve at six radial different positions in five different pericardial sacs. The grand mean of these values is

TABLE III The mechanical response to load in the unstrained state, measured by the slope at the origin of the stress–extension ratio curve for six differential radial positions and five different sacs. The grand mean is 0.224 ± 0.118

	Position					
Sac number	1	2	3	4	5	6
1	0.202	0.388	0.288	0.708	0.341	0.191
2	0.158	–	–	0.231	0.167	0.290
3	0.200	0.120	0.202	0.279	0.095	0.218
4	0.238	0.286	0.276	0.181	0.161	0.387
5	0.350	0.179	0.169	0.203	0.101	0.282

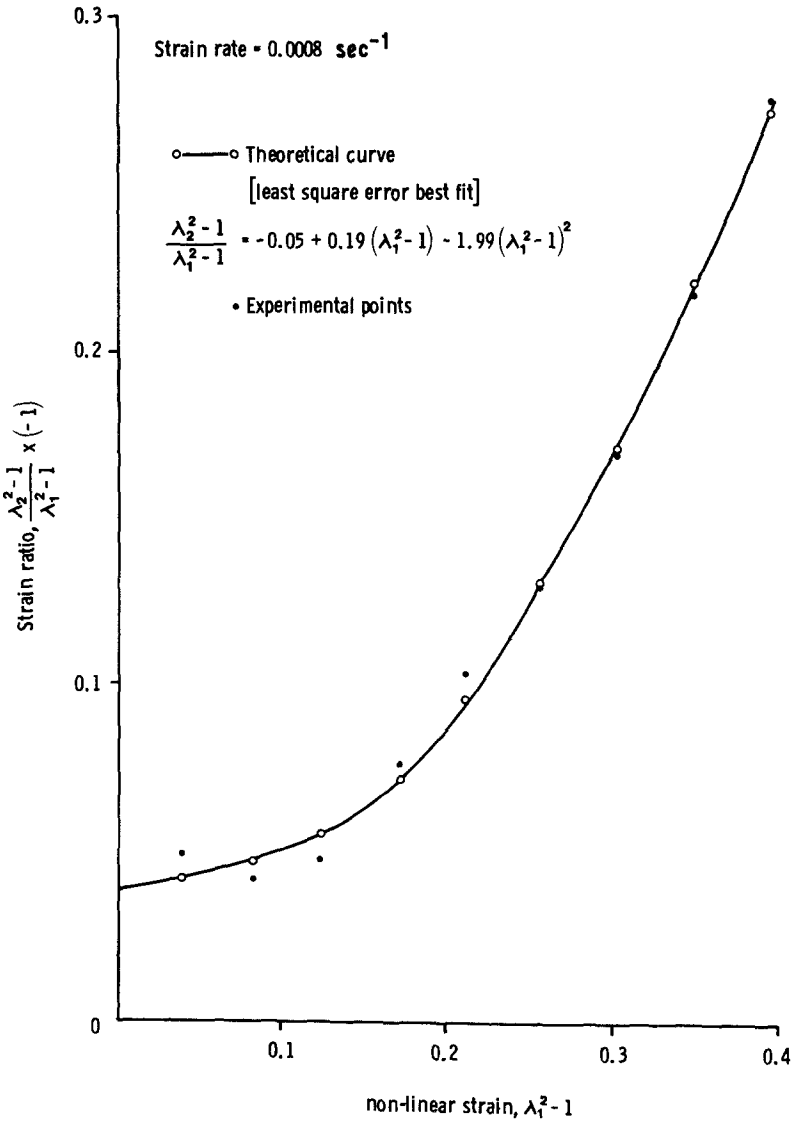

Figure 13 The variation of strain ratio $B_{22}/B_{11} = (\lambda_2^2 - 1)/(\lambda_1^2 - 1)$ with normal strain, $B_{11} = \lambda_1^2 - 1$, at "low" strain rate, 0.0008 sec^{-1}. The experimental points (•) lie on a quadratic truncation of the Taylor series expansion of normal strain, B_{11}, about the unstrained state (○——○). The effective Poisson's ratio (the value of the strain ratio as $\lambda_1 \to 1$) is + 0.05.

0.244 with a standard deviation of 0.118. Analysis of variance of these data shows that there is no significant difference in the response to load in the unstrained state from position to position in any sac or from sac to sac in any position.

The mean of the slopes at the origin of the stress–extension ratio curve of eight specimens cut at random from two further sacs was 0.286 with a standard deviation of 0.12. There is no significant difference (student *t* test) between the grand mean of the 28 specimens cut radially to the pericardium apex at six different positions in five sacs and the eight specimens cut in random directions from two further sacs.

5. Discussion

The desire to understand the behaviour of soft biological tissue when it is subjected to external forces has resulted in a substantial literature devoted to tissue characterization. Material scientists and bioengineers in the late 1950s and early 1960s applied engineering test procedures to skin in an effort to assist and provide information for the pragmatic approach adopted by the plastic

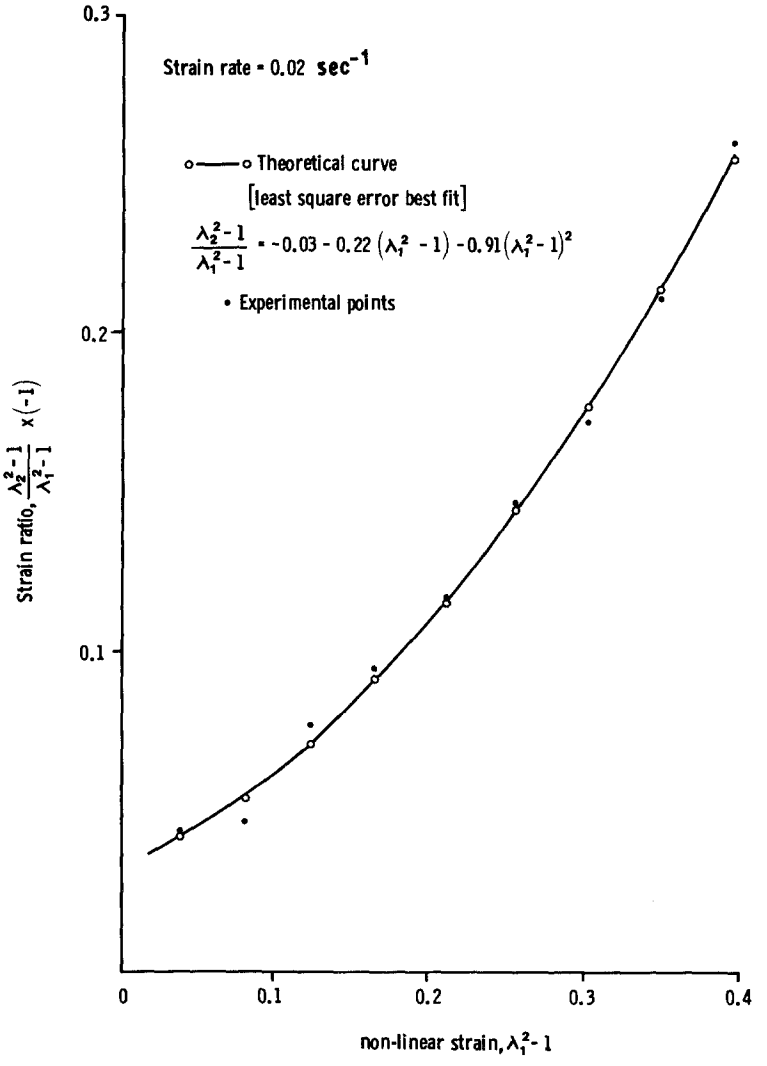

Figure 14 The variation of strain ratio $B_{22}/B_{11} = (\lambda_2^2 - 1)/(\lambda_1^2 - 1)$ with normal strain, $B_{11} = \lambda_1^2 - 1$, at "high" strain rate, 0.02 sec^{-1}, for the same specimen used for the "low" strain rate displayed in Fig. 13. Again the experimental points (•) lie on a quadratic truncation of the Taylor series expansion of normal strain, B_{11}, about the unstrained state (o——o). The effective Poisson's ratio is + 0.03 at the "high" strain rate compared with + 0.05 at the "low" strain rate.

surgeon during reconstructive surgery. Since that time the development of bioprosthetic devices, especially in heart valve replacement and by-pass grafts, have initiated intensive research programmes of material treatment and characterization.

The majority of investigations that have been reported can be criticised under three major headings:

1. the mechanical characterization is usually independent of the circumstances in which the tissue is used;

2. the region of applicability of the model formulation employed to characterize the tissue is not appropriate to the actual behaviour of the tissue;

3. the assessment is qualitative or relies on curve fitting techniques without physical or biological foundation.

All real materials lie somewhere in the spectrum between an idealized elastic solid and an idealized viscous fluid [23]. Rigid bodies and inviscid fluids are special cases of these two idealizations. The conditions to which the material is subjected often dictates the observed behaviour. The observations suggest at what point in the spectrum of idealizations the material behaviour caused by those

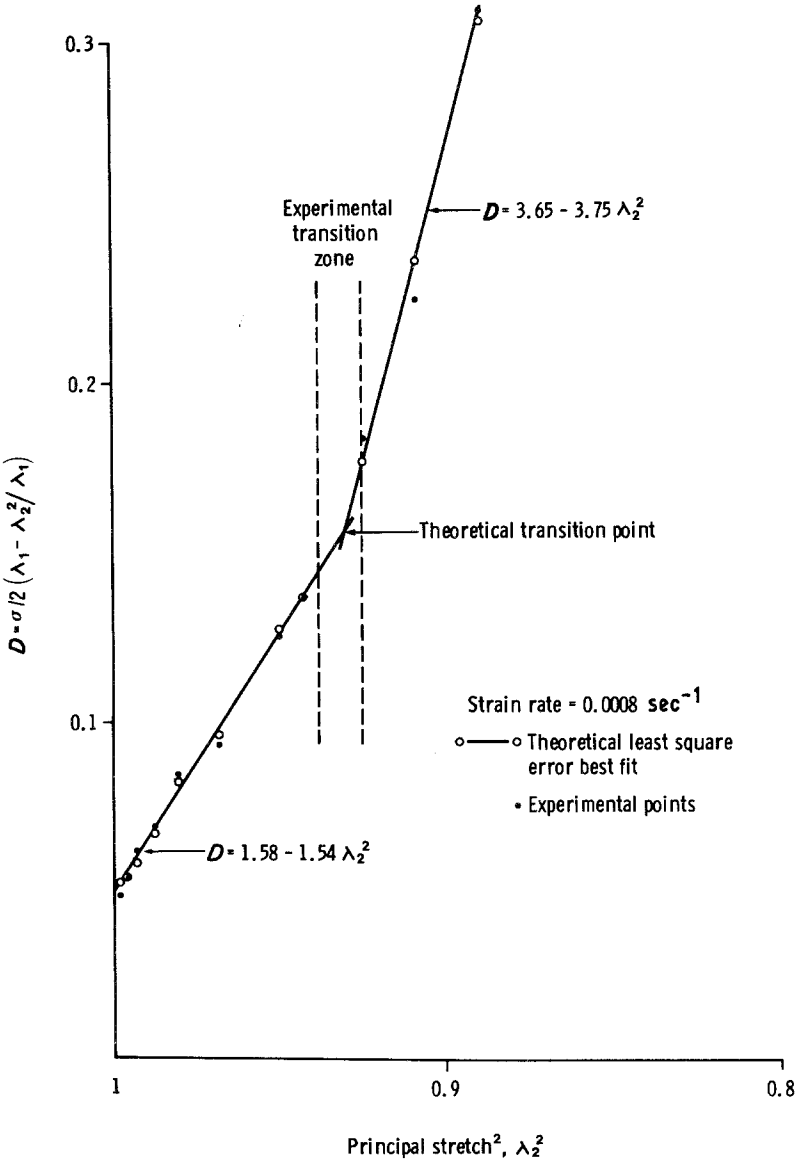

Figure 15 The variation of the strain energy differential, $D = \sigma/2\ (\lambda_1 - \lambda_2^2/\lambda_1)$ with the square of the contraction ratio, λ_2^2, at low strain rate, 0.0008 sec^{-1}. The experimental points (•) lie on two intersecting straight lines (○——○) with different slopes. This suggests that the tissue changes from one elastic material to a second elastic material as it is loaded. The theoretical transition point is at the intersection of the two lines. It is likely that in reality the transition takes place over a range of load and, consequently, a range of extension.

conditions should be placed. If the circumstances are changed then the material behaviour is changed and as a consequence the model idealization which best portrays this behaviour might well change. For example, a lump of ice which falls from a glacier onto a mountaineer below would be modelled as a rigid body when it strikes the unfortunate victim. However, the same mountaineer, if he were a glaciologist, may be quite happy modelling the ice as a fluid if he were interested in the movement of the glacier over a period of a year. This example and that related to "therapeutic putty" described in Section 1, suggest that time scales play an important part in the choice of a model which provides a good approximation of reality.

The second criticism arises from the use of models in a region of applicability for which they were not designed. For example, the infinitesimal theory of elasticity was constructed as a first order

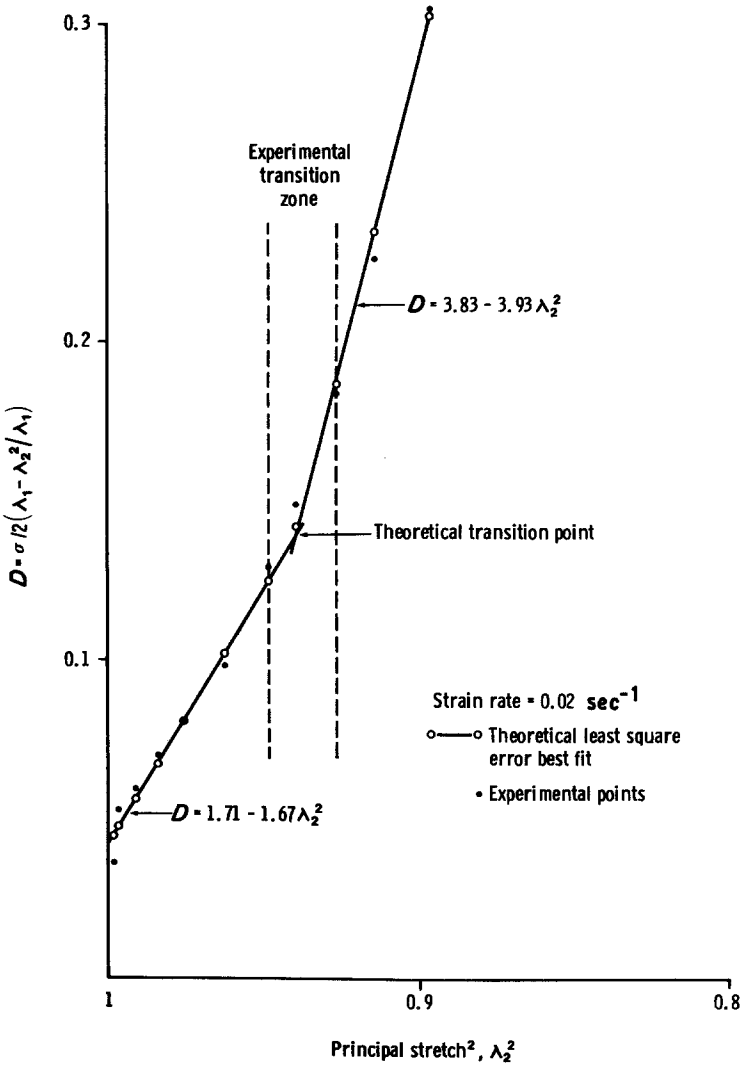

Figure 16 The variation of the strain energy differential, $D = \sigma/2\,(\lambda_1 - \lambda_2^2/\lambda_1)$ with the square of the contraction ratio, λ_2^2 at "high" strain rate, 0.02 sec^{-1}. Again the experimental points (•) lie on two intersecting straight lines (o——o) with different slopes. The slope of the straight line representing the initial elastic material changes from 1.54 at the "low" strain rate, 0.008 sec^{-1} (Fig. 15), to 1.67 at the "high" strain rate, 0.02 sec^{-1}. After the transition point the straight line representing the elastic material has a slope of 3.75 at the "low" strain rate (Fig. 15) which changes to 3.93 at the "high" strain rate.

linear continuum approximation to reality when the deformation gradients are considerably smaller than unity. When this condition no longer holds, as in the deformation of rubber, leather, skin and other biological tissues, the first order linear model breaks down. As a consequence the linear approximation to the actual strain measure is no longer valid. Although the change in length divided by the original length can still be measured it can no longer be considered as the strain measure. The uniaxial strain is non-linear in the extension ratio [21] and the engineering evaluation of strain is no longer appropriate. Furthermore, deductions of incompressibility from the comparison of elastic parameters that are only relevant in the infinitesimal theory are erroneous.

The same remarks apply to lumped parameter models that use a combination of springs and dash pots. The relationship between force and extension in a linear spring only applies to infinitesimal deformations. The linear viscous damping component of a dash pot only provides a first order theory for infinitesimally small strain rates.

The present study has used a continuum physics approximation of reality to model the behaviour of glutaraldehyde-fixed pericardium when it is subjected to uniaxial load. The enquiry was specifically directed at the operational mechanical properties of a bioprosthetic heart valve leaflet. For this reason a model which realistically considered the operational characteristics was required. Since typical fixed tissue relaxation times were of the order of years and a heart valve opens and closes approximately once a second, the

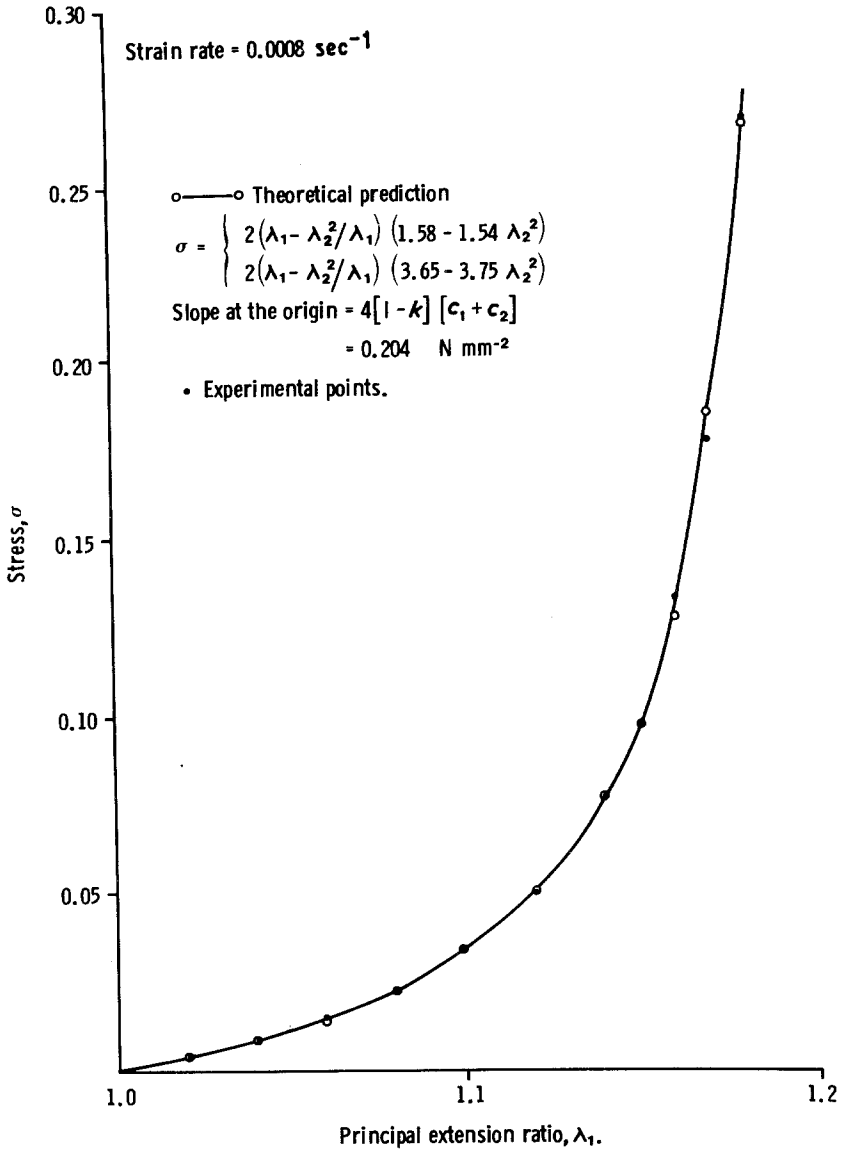

Figure 17 The variation of stress, σ, with extension ratio, λ_1, at the "low" strain rate, 0.0008 sec^{-1}. The experimental points (•) lie on (to a good approximation) the stress–extension ratio curve predicted by the theory (o——o). The slope of the curve at the origin, which provides a measure of mechanical response to uniaxial load in the unstrained state of the tissue, has a value 0.204 N mm^{-2}.

operational time scale is much shorter than the material relaxation time (see Fig. 5). As a consequence, stress relaxation is unlikely to have a dominant role in tissue behaviour in a heart valve.

Although energy was lost during the initial loading and unloading cyclic, stability of cycle with only small energy losses were observed after about eight cycles (Fig. 6). For this reason energy dissipation is unlikely to play an important role in short-term tissue behaviour in the valve leaflet. Moreover, the stress induced by loading was not altered substantially by varying the strain rate over a wide range.

These observations suggest that in the circumstances pertaining to heart valve performance the tissue behaviour is dominated by the characteristics associated with an ideal elastic material. This conclusion might, in the first instance, appear strange for a material that contains such a high percentage (approximately 75%) of unbound water. However, the experimental method essentially measures the deformation of the solid phase

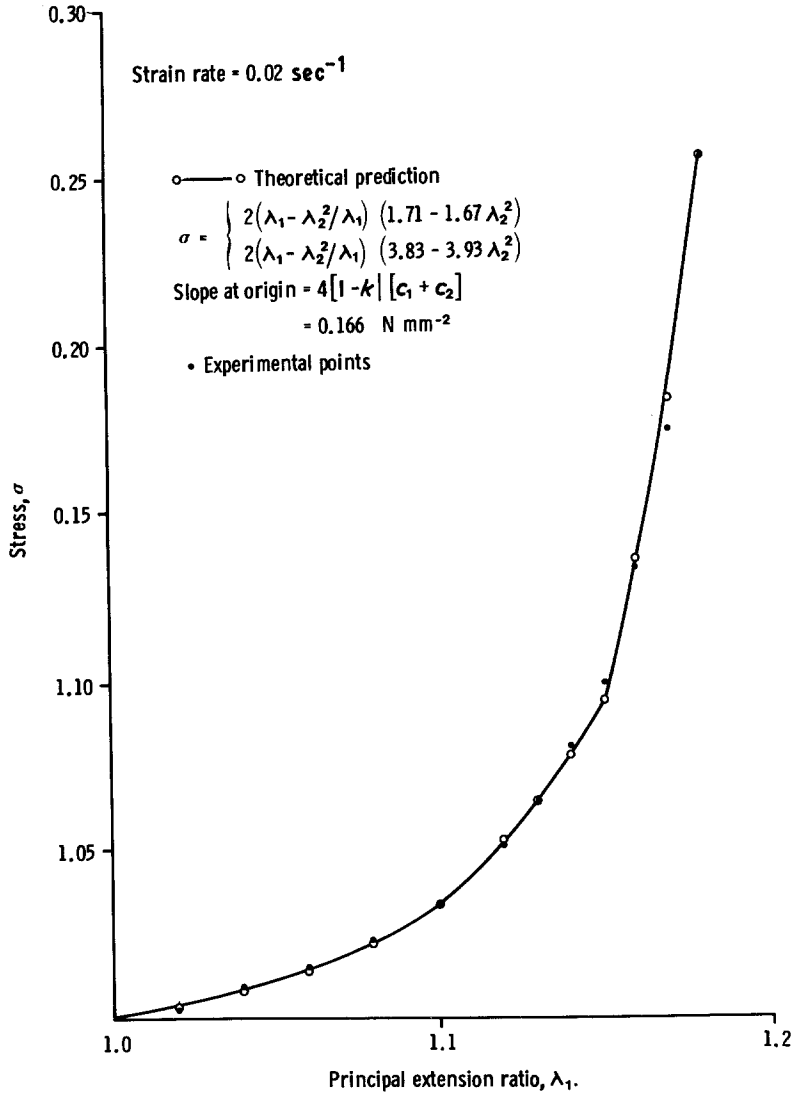

Figure 18 The variation of stress, σ, with extension ratio, λ_1, at the "high" strain rate, 0.02 sec^{-1}. The experimental points (•) lie on (to a good approximation) the stress–extension ratio curve predicted by the theory (○——○). The slope of this curve at the origin has a value 0.166 N mm^{-2}.

of the tissue while it is immersed in physiologically isotonic normal fluid. For this reason it is quite possible that it is the solid phase only and its interaction with the fluid phase (which includes the unbound water and ambient fluid) which displays the elastic characteristics. This suggestion is supported by a different response to load when the tissue is not immersed in saline (personal observations). The operating conditions of the valve leaflet are within a fluid ambient. For this reason they have been simulated on the test rig.

As a consequence it is not appropriate to use the argument that the high percentage of water (which under physiological forces is incompressible) renders the tissue incompressible. Nor can the comparison of bulk modulus and Young's modulus invoked by Carew *et al.* [9], be used to establish tissue incompressibility. The deformation of fixed pericardium, skin, and other tissue transcends the conditions of an infinitesimal elastic model. When the restraint of incompressibility is removed the principal contraction ratio, λ_3, can no longer be evaluated from the measured values of λ_1 and λ_2 in an uniaxial load test. As a consequence the evidence for anisotropy, the calculated value of λ_3 unequal to the measured value of λ_2,

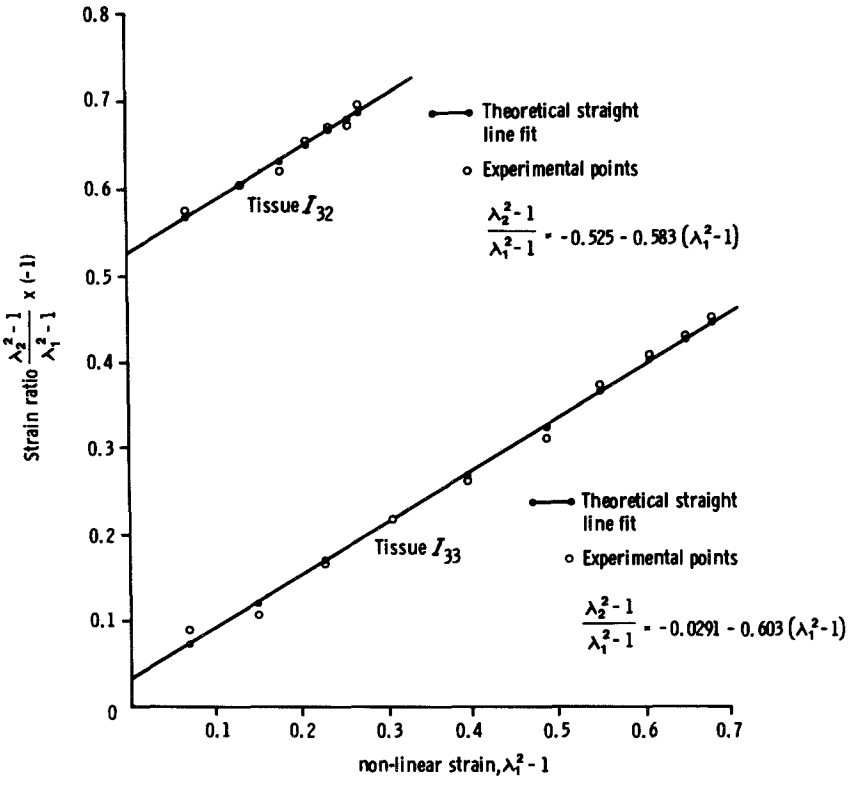

Figure 19 The variation of strain ratio, $B_{22}/B_{11} = (\lambda_2^2 - 1)/(\lambda_1^2 - 1)$, with the normal strain, $B_{11} = \lambda_1^2 - 1$, for two specimens cut at right angles to one another. Specimen I_{32} appeared to have a predominance of longitudinal collagen fibres while specimen I_{33} appeared to have the collagen fibres predominantly in the transverse direction. Experimental points (○) of both specimens lie on a linear truncation of the Taylor series expansion of normal strain, B_{11}, about the unstrained state (●——●). The effective Poisson's ratio of I_{32} is + 0.525, while that of I_{33} is + 0.029.

presented by Lanir and Fung [3] for rabbit skin, is no longer valid.

All materials display some degree of compressibility. Indeed, it has been shown that the expansion of rubber in uniaxial load is a necessary thermodynamic requirement [28]. Small volume changes during the extension of vulcanized rubber have been confirmed experimentally by Gee *et al.* [6].

In this study a compressible finite elastic model has been used. The measure of compressibility is provided by the value of the strain invariant of $I_3 = (V/V_0)^2$. Values of $I_3 > 1$ indicate an expansion of the material while values of $I_3 < 1$ indicate a contraction. Since $I_3 = \lambda_1^2\lambda_2^2\lambda_3^2$, it is the relative changes in the extension ratio, λ_1 and the contraction ratios λ_2 and λ_3, which determine the volume changes.

A further assumption of elastic isotropy has also been made. This restricts the material potential energy to a dependence on the strain invariants, I_1, I_2, and I_3, only. Furthermore the contraction ratio λ_2 and λ_3 should be equal over the whole deformation range in uniaxial load. Although attempts have been made to measure λ_3 by three different experimental methods, all have been fraught with technical problems and the results have been inconclusive. One of the major problems is the accuracy required to measure changes of less than 10% in a tissue of initial thickness of the order of 0.5 mm, when the tissue boundary may contain undulations approaching the dimensions that have to be measured. Methods using a microscope and ultrasound both suffer from this problem.

A method devised by Gee *et al.* [6] to measure volume changes in rubber by Archimedian principles has also been employed. Problems arising from fluid transfer during extension and its relationship to the deformation of the solid phase measured in the standard uniaxial load tests have, at the present time, clouded possible interpretation of the experimental observations. Of course vulcanized rubber immersed in fluid is not sub-

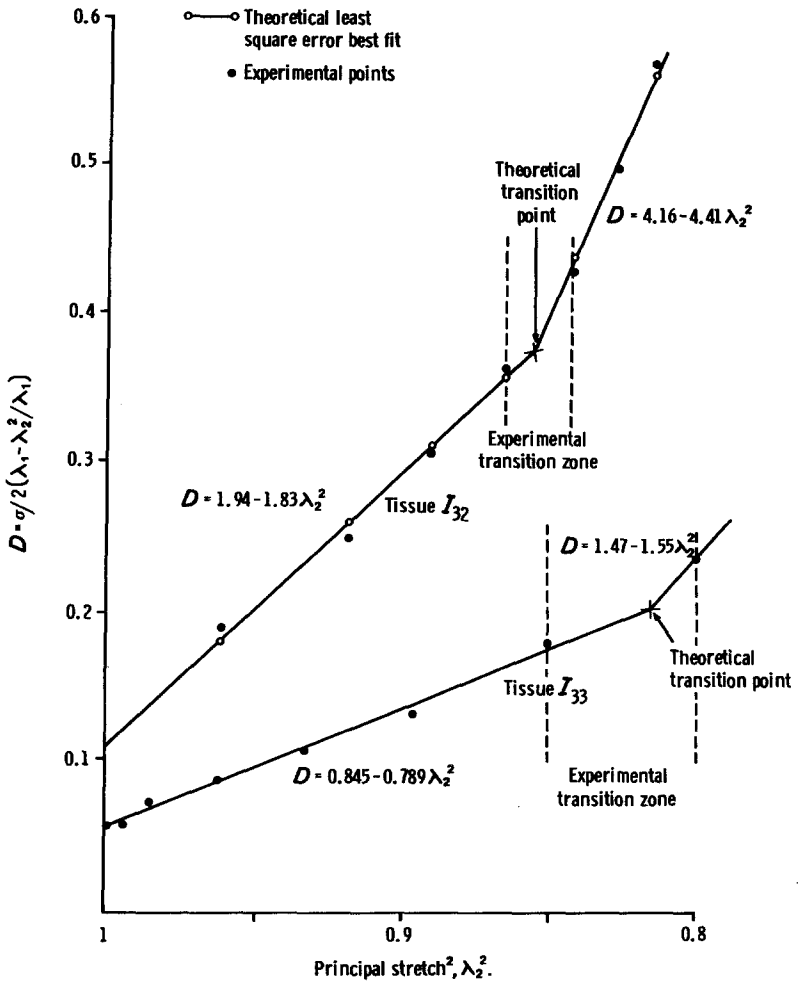

Figure 20 The variation of strain energy differential, $D = \sigma/2\ (\lambda_1 - \lambda_2^2/\lambda_1)$ with the square of the contraction ratio, λ_2^2 for the two specimens I_{32} and I_{33}. The experimental points (•) of both specimens lie on (to a good approximation) two intersecting straight lines (○——○). The transition points of the two specimens occur at different values of λ_2^2.

jected to fluid transfer into and out of the solid phase.

Although anisotropy has usually been an integral part of the discussion of the majority of studies of the mechanical behaviour of soft tissue this concept has never been incorporated, as far as the authors are aware, into a quantitative uniaxial finite elastic model. The continuum model averages all the molecular structure over a volume that can contain a number of collagen fibres of diameter 100 nm. Furthermore, it would appear that glutaraldehyde cross-linking which depends on collagen content, but is likely to be perpendicular to the 3α chain superhelices which constitute the pentafibrils, is the dominant determinant of mechanical behaviour changes [17].

As a consequence, although collagen content and direction may change the local material properties (on a macroscopic length scale), this may be simply due to biological variation rather than specific anisotropic properties. In the light of these considerations and since it is necessary to establish the mechanical properties (on average) for the tissue within the whole leaflet before they can be incorporated into a design procedure, an isotropic strain energy function was used. The mathematical simplicity which resulted from isotropy also makes this hypothesis attractive, although this was not the major consideration which influenced the choice of strain energy formulation.

Any idealized elastic model should contain the infinitesimal elasticity theory as a first order approximation. An extrapolation of this idea to

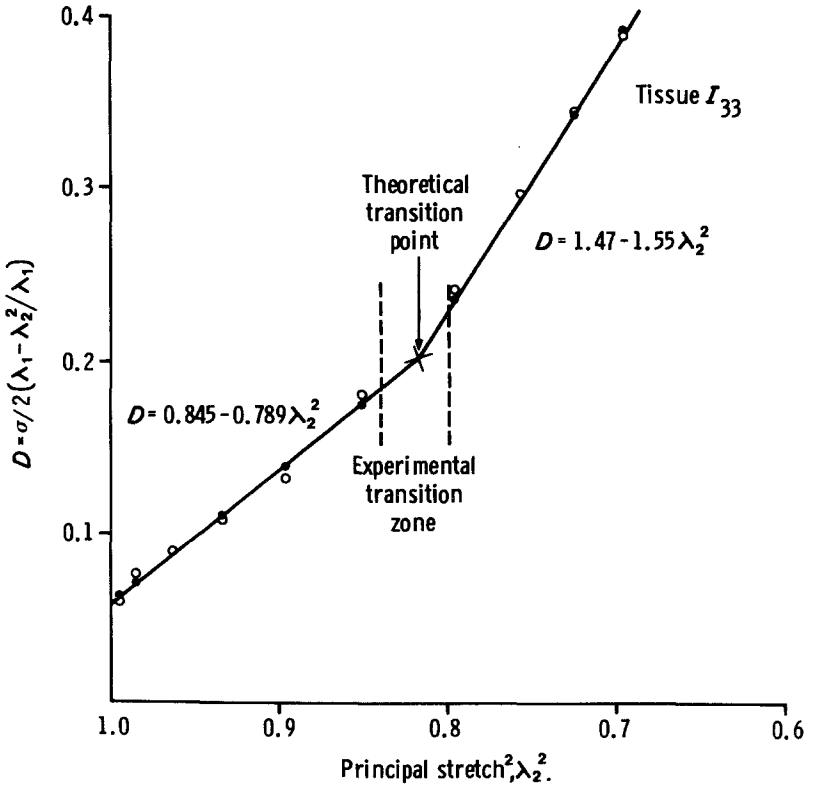

Figure 21 The variation of D with λ_2^2 for the specimen I_{33} alone. The experimental points (○) missing from Fig. 20 (dictated by the scale) have been included to show the increased degree of contraction of I_{33}, compared with I_{32}, for the same load.

the uniaxial load test suggests that the dependence of the strain ratio B_{22}/B_{11} on the normal finite strain B_{11} should be investigated. If B_{22}/B_{11} depends on B_{11} then in the limit of an infinitesimal deformation the strain ratio would be

$$\lim_{B_{11}\to 0} f(B_{11}) = \text{constant},$$

which can be equated with Poisson's ratio. Indeed the glutaraldehyde fixed pericardium displayed such a dependence. Expansion of the functional form of B_{11} in a Taylor series about the unstrained state allowed a polynomial approximation of $f(B_{11})$ to be constructed. A linear truncation was sufficient in some cases and it was never necessary to go beyond a quadratic approximation in all cases investigated (see Figs. 7 and 8).

Mathematical analysis of the homogeneous deformation produced by the uniaxial load showed that

$$D = \frac{\sigma}{2(\lambda_1 - \lambda_2^2/\lambda_1)} = \frac{\partial W}{\partial I_1} + \lambda_2^2 \frac{\partial W}{\partial I_2}.$$

As a consequence, a linear truncation in I_1 and I_2 of a Taylor series expansion of W about the equilibrium state suggests a linear relation between D and λ_2^2. At first glance the experimental values of D appear to vary non-linearly with λ_2^2. However, closer inspection reveals that the variation of D with λ_2^2 can be separated into two regions in both of which D and λ_2^2 are (to a good approximation) linearly related.

A physical interpretation of this phenomenon would be that the tissue behaves like an isotropic compressible elastic material which changes "phase" when a certain load is reached. The material potential energy induced by the load can be considered as a pair of intersecting surfaces in the four-dimensional space, W, I_1, I_2, I_3 (Fig. 23).

The equilibrium position of the initial elastic material is (0, 3, 3, 1), when the potential energy is zero for no deformation. The second elastic material would mathematically have a non-zero potential energy when $I_1 = 3$, $I_2 = 3$, $I_3 = 1$, but this position on the second potential energy surface is not physically realizable. As the material is loaded, the point (W, I_1, I_2, I_3) which represents the potential energy at a given deformation

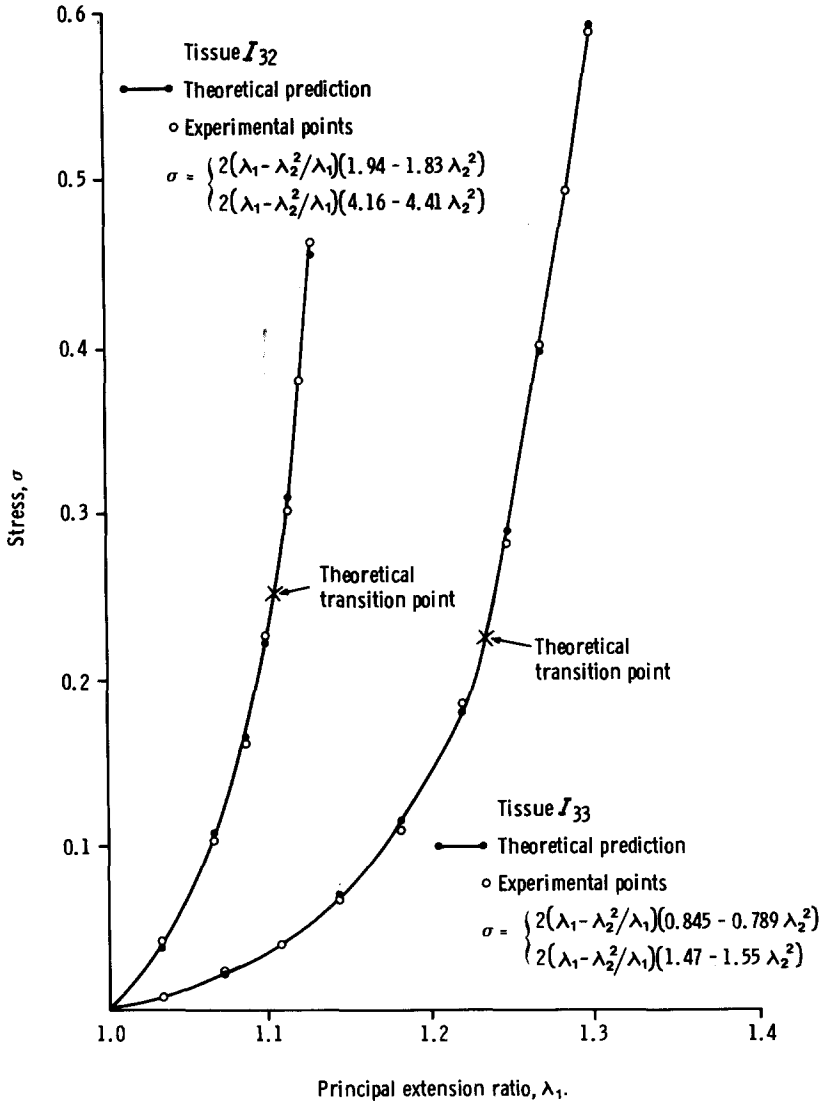

Figure 22 The observed and predicted variation of stress, σ, with principal extension ratio, λ_1, for the two specimens I_{32} and I_{33}. The experimental observations (○) lie on (to a good approximation) the stress–extension ratio curve predicted by the theory (●——●) in both specimens. The theoretical transition points occur at different extensions in the two specimens. Both transition points occur at substantially greater extensions than those associated with the "incubation period" [17].

moves along a four-dimensional space curve which meets the second potential energy surface at a specific potential energy/deformation point. This point in the continuum theory will depend inherently on the local material microstructure and how it is affected by the loading procedure. Further loading moves the point (W, I_1, I_2, I_3) on to the second potential energy surface (Fig. 23). The theory specifies a particular transition point; in practice the transition from one elastic material, with a specific strain energy, to a second elastic material, with a different strain energy but of the same functional form as the initial elastic material, will take place over a deformation range.

Once the variation of D with λ_2^2 has been categorized, the stress can be predicted at any extension. Figs. 12, 17, 18 and 22 show that agreement between prediction and experimental observation is excellent over the whole deformation range considered.

It is not yet clear how the different elastic potentials relate to changes in the tissue micro-

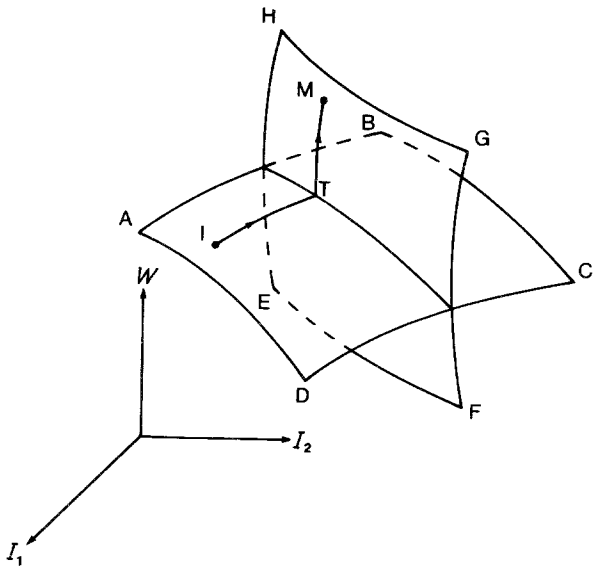

Figure 23 The schematic representation of the projection onto the plane I_3 = constant of the intersecting potential energy surfaces in the four-dimensional space, W, I_1, I_2, I_3. The projection of a four-dimensional surface on to a coordinate plane in four-dimensional space gives a surface in the resulting three-dimensional space. The surface ABCD represents the projected potential energy surface associated with the initial elastic material. The point I is the projection of the point (0, 3, 3, 1) onto the plane I_3 = constant. The curve IT represents the projection of the four-dimensional space curve on to I_3 = constant. The transition point is reached at T. At this stage in the deformation the space curve traced out by the point (W, I_1, I_2, I_3) moves on to a new potential energy surface. The projection of this surface on to I_3 = constant is EFGH. The point (W, I_1, I_2, I_3) now moves along a four-dimensional space curve, whose projection on to I_3 = constant is TM, until the maximum extension is achieved.

structure. Such a correlation awaits a future investigation. It has been suggested [17, 29–32] that the disappearance of collagen crimping in pericardium tissue signals the cessation of the high compliance region (referred to as the "incubation" region by Broom [17]) and the onset of rapid material stiffening with extension. The latter phenomenon has been explained by the uniaxial loading of straightened collagen fibres [17].

The evidence presented here (Fig. 22) suggests that the transition from one elastic potential to a second elastic potential occurs at larger extensions than might be associated with Broom's incubation region. However, since this region has only ever been described qualitatively, quantitative comparisons are difficult to make. Indeed, the material transition point is not reached at all in Fig. 11, yet the concomitant stress–principal extension curve, Fig. 12, has a characteristic soft tissue non-linear behaviour. If the rapid material stiffening region is associated purely with collagen fibre loading, irrespective of the accompanying molecular material constituents, then some form of transition would have been expected in Fig. 11.

The close agreement between experiment and theory allows the slope at the origin of the stress–extension ratio curve to be computed mathematically. In this way the mechanical response to load in the unstrained state may be determined. This allows a test for the elastic symmetries associated with the material.

Only statistical analysis can confirm whether qualitative appearances are indeed quantitative differences. Table IV shows that there is no significant difference in the mechanical properties from pericardial sac to pericardial sac; nor is there any significant difference in mechanical properties from position to position in an individual sac for specimens whose longitudinal lengths are in an apex radial direction.

There is no significant different between the mechanical properties of specimens cut at random and those cut in a specific direction. This experimental and statistical evidence suggests the pericardium behaves like an isotropic compressible

TABLE IV The analysis of variance from position to position and sac to sac for the statistics displayed in Table III. There is no significant difference between the mechanical response to load from sac to sac or from position within a sac (F test)

Source of variation	Sum of squares	Degrees of freedom	Estimated variation	F
Residual between sacs	0.092	4	0.023	1.84
Residual between position in a sac	0.061	5	0.012	1.02
Remaining Residual	0.225	18	0.013	
Total sum of squares	0.378	27		

material. The assertions that bovine pericardium is anisotropic have not been based on quantitative evaluation of the material response to load, in the unstrained state in different directions. In fact the elastic symmetries of the bovine pericardium have not been investigated by Broom [17] at all.

In conclusion, this study has shown that glutaraldehyde fixed pericardium can be modelled, to a good approximation, as an isotropic compressible elastic material that undergoes a transition to a second elastic material governed by a potential energy function of different magnitude but the same functional form as that associated with the initial elastic material. There is no experimental evidence of anisotropy. If the operational stress in bioprosthetic valve leaflets is required for design requirements then all of the above characteristics should be incorporated in the subsequent analysis.

This study also suggests that quantitative assessment of other soft biological tissue may require re-evaluation, depending on the conditions to which it will be subjected.

Acknowledgements

The authors acknowledge the invaluable assistance given by Dr Pat Lawford in numerous discussions about the pericardium microstructure. One of us (CLD) acknowledges the receipt of a SERC studentship during the period of this research. We acknowledge the assistance of Mrs Dorothy Day in preparing the manuscript.

References

1. T. GIBSON, "Proceedings of the Symposium on Biomechanics and related Bioengineering topics", edited by R. M. Kenedi (Pergamon, London, 1965) pp. 129-34.
2. R. M. KENEDI, T. GIBSON and M. ABRAHAMS, *Hum. Factors* **5** (1963) 525.
3. Y. LANIR and Y. C. FUNG, *J. Biomechanics* **1** (1974) 171.
4. A. VIIDIK, in "Biology of Collagen", edited by A. Viidik and J. Vaust (Academic Press, New York and London, 1980) pp. 237-55.
5. R. S. RIVLIN and D. W. SAUNDERS, *Phil. Trans. Roy. Soc. (A)* **243** (1951) 251.
6. G. GEE, J. STERN and L. R. G. TRELOAR, *Trans. Faraday Soc.* **50** (1950) 1101.
7. R. M. KENEDI, T. GIBSON and C. H. DALY, in "Proceedings of the Symposium on Biomechanics and related Bioengineering topics," edited by R. M. Kenedi (Pergamon, London, 1965) pp. 147-58.
8. Y. C. FUNG, *Amer. J. Physiol.* **213** (1967) 1532.
9. T. E. CAREW, R. N. VAISHNAV and D. J. PATEL, *Circ Res.* **23** (1968) 61.
10. D. J. PATEL and D. L. FRY, *ibid.* **24** (1969) 1.
11. R. N. VAISHNAV, J. T. YOUNG, J. T. JANICKI and D. J. PATEL, *J. Biophys.* **12** (1972) 1008.
12. E. G. TICKNER and A. H. SACKS, *Biorheology* **4** (1967) 151.
13. M. M. BLACK, P. J. DRURY and W. B. TINDALE, *J. Roy. Soc. Med.* **76** (1983) 667.
14. N. D. BROOM, *J. Thorac. Cardiovasc. Surg.* **75** (1978) 121.
15. *Idem, ibid.* **76** (1978) 202.
16. *Idem, Connect. Tissue. Res* **6** (1978) 37.
17. *Idem, J. Biomechanics* **10** (1977) 707.
18. S. W. RABKIN and P. H. HSU, *Amer. J. Physiol.* **229** (1975) 896.
19. G. BATCHELOR, "An Introduction to Fluid Dynamics" (Cambridge University Press, 1967).
20. A. E. GREEN and J. E. ADKINS, "Large elastic deformations and non-linear continuum mechanics" (Oxford University Press, 1970).
21. R. J. ATKIN and N. FOX, "An Introduction to the Theory of Elasticity", (Longman Mathematical Texts, London and New York, 1980).
22. E. A. TROWBRIDGE, *Clin. Phys. Physiol. Meas.* **3** (1982) 249.
23. A. C. PIPKIN, "Lectures on Viscoelastic Theory" (Applied Mathematical Sciences, Springer-Verlag, New York, 1972).
24. K. LANGER, *S. B. Akad. Wiss. Wien* **44** (1961) 19.
25. A. J. M. SPENCER, "Continuum mechanics" (Longman Mathematical Texts, London and New York, 1980).
26. G. E. MASE, "Theory and problems of continuum mechanics", Schaum's outline series (McGraw-Hill, London, New York, 1980).
27. R. C. HAUT and R. W. LITTLE, *J. Biomechanics* **5** (1972) 423.
28. G. GEE, *Trans. Faraday Soc.* **42** (1946) 585.
29. M. ABRAHAMS, *Med. Biol. Engng.* **5** (1967) 433.
30. A. VIIDIK, *Z. Anat. Entw-gesch.* **136** (1972) 204.
31. *Idem*, in "International Review of Connective Tissue Research", Vol. VI, edited by D. A. Hall and D. S. Jackson (Academic Press, New York and London, 1973) pp. 127-215.
32. J. H. EVANS and J. C. BARBENEL, *Equ. vet. J.* **7** (1975) 1.
33. P. LAWFORD, personal communication (1983).

Received 23 February
and accepted 9 March 1984